energies

MDPI

Article

Monitoring and Diagnosing Faults in Induction Motors' Three-Phase Systems Using NARX Neural Network

Valbério Gonzaga de Araújo [1,†], Aziz Oloroun-Shola Bissiriou [2,†], Juan Moises Mauricio Villanueva [3,†], Elmer Rolando Llanos Villarreal [4,†], Andrés Ortiz Salazar [2,*,†], Rodrigo de Andrade Teixeira [2,†] and Diego Antonio de Moura Fonsêca [2,†]

1 Federal Institute of Education, Science and Technology of Rio Grande do Norte (IFRN), Canguaretama 59190-000, RN, Brazil; valberio.araujo@ifrn.edu.br
2 Department of Computer Engineering and Automation, Federal University of Rio Grande do Norte (DCA-UFRN), Natal 59072-970, RN, Brazil; aziz.bissiriou.b07@ufrn.edu.br (A.O.-S.B.); rodrigoandradeteixeira@gmail.com (R.d.A.T.); diegomoura@dca.ufrn.br (D.A.d.M.F.)
3 Department of Electrical Engineering, Center for Alternative and Renewable Energies—CEAR, Federal University of Paraíba (CEAR-UFPB), João Pessoa 58051-900, PB, Brazil; jmauricio@cear.ufpb.br
4 Department of Natural Sciences, Mathematics, and Statistics, Federal Rural University of Semi-Arid (DCME-UFERSA), Mossoró 59625-900, RN, Brazil; elmerllanos@ufersa.edu.br
* Correspondence: andres@dca.ufrn.br
† These authors contributed equally to this work.

Abstract: Three-phase induction motors play a key role in industrial operations. However, their failure can result in serious operational problems. This study focuses on the early identification of faults through the accurate diagnosis and classification of faults in three-phase induction motors using artificial intelligence techniques by analyzing current, temperature, and vibration signals. Experiments were conducted on a test bench, simulating real operating conditions, including stator phase unbalance, bearing damage, and shaft unbalance. To classify the faults, an Auto-Regressive Neural Network with Exogenous Inputs (NARX) was developed. The parameters of this network were determined through a process of selecting the best network by using the scanning method with multiple training and validation iterations with the introduction of new data. The results of these tests showed that the network exhibited excellent generalization across all evaluated situations, achieving the following accuracy rates: motor without fault = 94.2%, unbalanced fault = 95%, bearings with fault = 98%, and stator with fault = 95%.

Keywords: artificial intelligence; failure classification; induction motor; artificial neural network

Citation: Araújo, V.G.d.; Bissiriou, A.O.-S.; Villanueva, J.M.M.; Villarreal, E.R.L.; Salazar, A.O.; Teixeira, R.d.A.; Fonsêca, D.A.d.M. Monitoring and Diagnosing Faults in Induction Motors' Three-Phase Systems Using NARX Neural Network. *Energies* **2024**, *17*, 4609. https://doi.org/10.3390/en17184609

Academic Editor: K. T. Chau

Received: 18 June 2024
Revised: 19 July 2024
Accepted: 24 July 2024
Published: 13 September 2024

1. Introduction

Three-phase induction motors (TIMs) are widely used as the driving force in various industrial applications, ranging from clean environments, such as in the food industry, to more challenging or aggressive environments in heavy installations, such as the petrochemical and metal-processing industries. They are preferred due to several advantageous characteristics, including low cost, robustness, high reliability, and constructive simplicity. Many studies focus on improving the design, dynamic performance, and these machines' efficiency [1]. Three-phase induction motors are electromechanical energy converters that transform electrical input power from the power supply into mechanical output power delivered to the load, and despite inherent losses in the process, they remain highly efficient. In Brazil, the industrial sector demands 31.6% of the domestic electricity supply, with electric motors consuming 68% of this energy, highlighting the significant potential for energy savings [2].

Motors are subject to unavoidable stresses in practice. Environmental, thermal, mechanical, magnetic, and electrical variations can cause certain faults in motors. These faults,

if not detected and eliminated in time, can lead to an unexpected breakdown and stoppage of the motor and, consequently, a reduction in the industry's efficiency and possible damage to equipment or people nearby [3].

According to the work in [4], approximately 40–50% of induction motor failures are related to mechanical defects. These failures can be classified into two main categories: (i) rolling element bearing damage and (ii) eccentricity. Bearing failures can manifest as defects in the outer race, inner race, balls, or rollers. Factors such as vibrations, internal stresses, inherent eccentricity, and bearing currents significantly influence the development of these failures. Furthermore, temperature is a significant contributing factor to bearing failure. It is therefore recommended that the temperature does not exceed the predetermined limits under nominal load conditions. As stated in reference [5], it is crucial not to neglect voltage imbalance in the power supply. This imbalance leads to a significant increase in stator currents, causing copper losses and constituting one of the main sources of temperature rise. Conventional induction motors are designed to operate in ambient temperatures of up to 40 °C. Therefore, temperatures exceeding this standard limit can result in thermal stress.

Fault diagnosis can be carried out using traditional noninvasive techniques. These strategies generally involve analyzing parameters such as vibration, voltage, current, torque, and speed [6].

Since the installation of several backup motor units is not economical, monitoring induction machines is essential to ensure safe operation and maintain product quality. Therefore, the monitoring, detection, classification, and diagnosis of faults are crucial for keeping equipment in good operating condition. There are two main categories of techniques for identifying machine faults: invasive and noninvasive, with noninvasive techniques generally being preferred. Artificial intelligence (AI) systems have been proposed for the noninvasive detection of machine faults [7].

Among the conventional methods widely used in the literature, the Time–Frequency Domain Analysis (TFDA) method stands out for the detection of faults in induction motors. For instance, in [8], an approach based on the Fast Fourier Transform (FFT) is reported, which aims to analyze the motor's vibration and current signature for fault detection. This approach proposes to detect both mechanical faults, such as bearing damage, and electrical faults, such as unbalanced voltage supply or single-phase conditions. In this context, the authors employ Fourier spectral analysis via the FFT to extract features sensitive to the presence of faults. Mechanical and electrical faults imprint specific frequency characteristics on the current and vibration spectrum, which can be used for fault detection by comparing the amplitude of certain frequency components under normal and faulty conditions. Also, a discrete wavelet transform is employed in [9] for the detection of inter-turn short-circuit (ITSC) faults in induction motor stators. However, these Time–Frequency-Domain-based methods can be highly sensitive to noise in the measured signals, as high-frequency noise can mask actual faults, complicating accurate detection.

Fault-diagnosis methods using computational intelligence, through techniques based on Artificial Neural Networks (ANNs), Fuzzy Inference Systems (FISs), and Genetic Algorithms (GAs), have shown promising results in detecting and identifying faults in three-phase induction motors.

The objective of this work is to use artificial intelligence techniques to diagnose and classify faults related to shaft imbalance, stator damage, and bearing damage in three-phase induction motors. This will be performed by monitoring current, vibration, and temperature signals. The main aim is to achieve greater precision in the diagnosis of these mechanical and electrical faults, harnessing the power of artificial intelligence to analyze data and identify patterns, which can result in more assertive and effective interventions in the preventive and corrective maintenance of the equipment. This paper proposes to explain four distinct test scenarios that are important for identifying the motor operating conditions. These scenarios are fundamental because they allow for the collection of engine signal readings in different situations, which is essential for validating the proposed method.

This paper is organized as follows. Section 1 presents the introduction. Section 2 presents the preliminaries. The theoretical background is presented in Section 3. Section 4 describes the materials and methods used. Section 5 presents the results obtained. Section 6 shows the discussions, and Section 7 concludes this paper.

2. Preliminaries

Monitoring faults in three-phase induction motors has aroused the interest of many researchers, resulting in a growing number of papers on the subject. This section presents some of these studies.

In [10], observing the low dynamic processing capacity as the main limitation of modeling methods based on feed-forward neural networks for detecting turn faults in the stator winding of an induction motor, the authors implemented a diagonal recurrent neural network based on an online turn fault-detection approach. In this case, two diagonal recurrent neural networks were used, one to estimate the severity of the fault and the other to determine the exact number of times it occurs. To make the network more accurate, an adaptive dynamic backpropagation algorithm was used. The results demonstrated that the diagnostic model based on a diagonal recurrent neural network accurately determines shorted turns and is more effective than the diagnostic model based on a direct neural network.

In [11], a support vector machine algorithm based on artificial immunity for diagnosing faults in induction motors was proposed. In this paper, the stator and rotor faults in an induction motor were detected using the three-phase motor currents. The healthy and faulty motor conditions were classified in combined phase space using an immunity-based SVM algorithm. The optimal SVM parameters are obtained using a clonal selection algorithm. Besides, the motor currents were taken in a real experimental setup, and successful results were obtained.

In [12], an approach to the problem of fault detection and isolation in three-phase induction motors using recurrent neural networks and dynamic Bayesian modeling was presented. The idea was to create a neural model to emulate the system's normal behavior and additional models to emulate various fault conditions. The neural models are placed in parallel with the system to be monitored, and fault detection is achieved by comparing the outputs of the neural models with the actual outputs of the system. The neural network was trained using the stochastic simultaneous perturbation approximation (SPSA). Fault classification was based on a simple threshold test of the residuals, which were formed by subtracting each neural model output from the corresponding real system output. A hybrid system that used data collected by vibration and current sensors for the early and efficient detection of incipient faults in three-phase induction motors was used. The system employed advanced vibration and current analysis techniques, including multiresolution analysis with wavelet, Fourier transform, and fuzzy logic for fault classification.

In [13], an approach for monitoring the operating conditions of three-phase induction motors based on extracting the characteristics of a vibration signal obtained with a MEMS accelerometer is investigated. The authors extracted data from the decomposition of the vibration signal by the Haar transform and through the fractal dimension, which were employed to train an ELM Neural Network.

In [14], strategies were introduced for diagnosing and predicting faults and failures in induction motors as an alternative tool to traditional models for detecting short-circuit faults between stator turns, rotor bar breakage, and bearings under normal operating conditions using Artificial Neural Networks with a radial basis function. The current signals of a three-phase induction motor under various fault conditions were treated and processed using synchronous axis transforms. These signals were classified using the RBF network, indicating the samples referring to the signals without faults and with the three types of faults. It was found that the network presented 1.33% error for loads of 1 Nm, 2 Nm, and 3 Nm and zero error for loads of 4 Nm and 5 Nm. The experimental results demonstrated that the employed methodology successfully classified the signals.

In [15], a proposal for a three-phase induction motor signature analysis technique to diagnose faults between stator turns was considered. This technique employs a wavelet transform and a support vector machine as a classification tool. The proposed technique was based on the stator current analysis under healthy and faulty conditions. The wavelet decomposition, based on a lifting algorithm, was implemented in the system with an ARM processor to reduce implementation costs.

In [16], a study was presented on fault-diagnosis techniques for three-phase induction motors, focusing on industrial applications. In this paper, various methods were explored, including current signature analysis, mechanical vibration, acoustic vibration, energy efficiency, and air gap torque. The authors also employed the Fast Fourier Transform and the multiresolution analysis with a wavelet. Mechanical faults were effectively diagnosed using vibration analysis and sound analysis of the noise emitted by the motor. MRA analysis proved to be efficient for practically all types of faults associated with various types of failure. The torque spectral analysis in the air gap and sound acquisition by MRA proved to be excellent alternatives for detecting broken bars. For bearing fault detection, spectral analysis combined with MRA analysis for vibration signals proved to be the most suitable approach. The mechanical vibration fault diagnosis via spectral analysis also proved to be the best option for unbalancing for different applied loads.

In [17], an alternative method for detecting faults in the bearings of three-phase induction motors directly connected to the mains was proposed. This method utilizes the amplitudes of voltage and current magnitudes in the time domain, eliminating the need for signal manipulation and transformation. Experimental data collected in the laboratory facilitated the establishment of an ANN topology capable of better interpreting the signals used as input. This approach obtained satisfactory results with over 99% accuracy for cross-validation and around 97% for validation with data acquired from machines not used in the training process. The proposed network was the Multilayer Perceptron (MLP), consisting of two hidden layers with seven neurons each, plus the output layer with two neurons for classification. Supervised training was also applied with the backpropagation method plus the Levenberg–Maquardt (LM) algorithm, stipulating the Mean Square Error (MSE) as the stopping criterion.

In [18], a comprehensive review of AI algorithms for diagnosing faults in rotating machines is presented from both a theoretical and an industrial application standpoint. The methods presented include k-nearest neighbor, Naïve Bayes, support vector machine, Artificial Neural Network, and deep learning, which are discussed as potential approaches for fault diagnosis. As AI techniques continue to mature, it is anticipated that they will remain a valuable and powerful tool for diagnosing faults in rotating machinery.

In [19], continual learning is introduced as a promising technique that allows intelligent motor fault-diagnosis models to extend new diagnosable fault classes without costly training from scratch.

In [20], a two-step approach for fault detection and classification in electric motor drives used in wind turbine pitch systems is presented. The proposed methodology is suitable for application in offshore wind farms, both for electrical pitch systems driven by induction motors and by permanent magnet synchronous motors. The adopted strategy involved measuring the three-phase current signal of the motors in the pitch drives, using these measurements to detect faults and feed a classifier based on support vector machines (SVMs). The proposed method was validated in an internal test environment of the pitch drive system. The SVM classifier demonstrated an overall accuracy of 98% in predicting fault classes in the training set and 96.5% in predicting fault classes in the test set.

Despite the reliability generally associated with three-phase induction motors, they are still susceptible to a variety of faults from both mechanical and electrical sources during motor operation. This scenario presents a significant challenge for the industry, requiring the ongoing development of techniques capable of monitoring and diagnosing these faults at an early stage.

Several approaches have been proposed to detect these issues, all with the clear objective of contributing to more effective maintenance and, consequently, reducing production losses. In many investigations, artificial intelligence has been highlighted by various authors as a crucial tool in systems modeling. Among the various artificial intelligence techniques, machine learning stands out in the development of fault-classification systems, as corroborated by the works cited.

It can be concluded that the topic has not yet reached its full maturity, presenting numerous opportunities for exploration, particularly in the field of deep learning through Artificial Neural Networks. Ongoing research and development in this area are crucial for enhancing the reliability and efficiency of three-phase induction motors. This, in turn, will contribute to the safer and more economical operation of these essential systems across various industrial applications.

3. Theoretical Background

This section presents fundamental concepts and theoretical aspects related to the development of this work. It includes an overview of three-phase induction motors, a discussion of typical faults in these motors, and a brief description of AI techniques applied to fault detection in motors.

3.1. Three-Phase Induction Motors

An electric motor is a machine designed to transform electrical energy into mechanical energy. Among the various types of motors, the induction motor is the most widely used as it offers a combination of advantages when it comes to the use of electrical energy. The main advantages of induction motors are their low cost, ease of transportation, cleanliness, and simplicity of control. These advantages are derived from the simple construction, low cost, and great versatility in adapting to loads of the most diverse types, as well as better efficiency yields [21]. A large proportion of the industrial sector consists of electric motors, including both direct current (DC) and alternating current (AC) motors. These motors are essential for the functioning of industrial processes [22].

The induction machine mainly functions as a motor and can be categorized as either three phase or single phase (two phase). Single-phase models use specialized devices to achieve the starting torque. A key feature is its independence from a DC source, making it robust, versatile, and cost-effective. These motors come in various power capacities, from large-scale to fractional power applications. Furthermore, the lack of brushes reduces the need for maintenance.

Figure 1 shows the main components of a TIM.

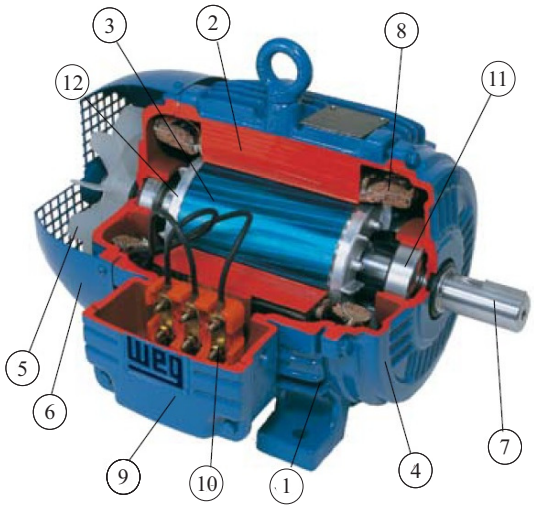

Figure 1. TIM components.

Estator:

- Housing (1)—the supporting structure of the assembly; it is made by employing robust construction with cast iron, steel, or injected aluminum and is corrosion-resistant and has fins.
- Core plates (2)—the plates are made of magnetic steel and are heat-treated to reduce losses of iron to a minimum.
- Three-phase winding (8)—Three equal sets of coils, one for each phase. These coils form a three-phase system and are connected to the three-phase supply network.

Rotor:

- Shaft (7)—Transmits the mechanical power developed by the engine. They are heat-treated to avoid problems such as warping and fatigue.
- Core plates (3)—the plates have the same characteristics as the stator plates.
- Short-circuit bars and rings (12)—made of aluminum die cast in a single piece.

Other parts of the TIM:

- Cover (4).
- Fan (5).
- Deflector cover (6).
- Junction box (9).
- Terminals (10).
- Bearings (11).

3.1.1. Working Principle

Induction motors, available in single-phase or three-phase configurations, are named after the power transfer principle from the stator's primary winding to the rotor. This transfer happens due to the relative movement between the magnetic field generated by the stator winding and the rotor conductors, inducing a voltage in the rotor. This principle underlies the fundamental dynamics behind the efficient and versatile operation of induction motors, which are crucial in many industrial and commercial applications [23].

3.1.2. Synchronous Speed

The motor synchronous speed is defined by the rotational speed of the motor rotating field, which depends on the number of poles (p) of the motor and the frequency (f) of the network, in hertz. Windings can be constructed with one or more pairs of poles, which are distributed alternately (north and south) along the periphery of the magnetic core. The rotating field travels through a pair of poles (p) each cycle. Thus, as the winding has poles or p pairs of poles, the field speed will be:

$$n_s = \frac{120 \cdot f}{p} \quad (1)$$

n_s — speed (rpm) under nominal conditions.
f — frequency of the electrical supply voltage (Hz).
p — total number of poles per phase.

3.1.3. Slip

The induction motor is also referred to as an asynchronous motor, given that the operational speed of the shaft is slightly below the synchronous speed. This small difference occurs because the rotor speed is slightly lower than the speed of the rotating magnetic field. This difference, called slip, increases with each rise in the mechanical load on the shaft.

Slip is the difference between the motor speed n and the synchronous speed ns, which can be expressed in rpm as a fraction of the synchronous speed or as a percentage of it:

$$S_{rpm} = n_s - n \quad (2)$$

$$S = \frac{(n_s - n)}{n_s} \times 100 \tag{3}$$

S — slip.
n_s — rotating magnetic field speed (rpm).
n — nominal speed (rpm). - nominal speed (rpm).

3.1.4. Rated Speed

The nominal speed of the motor (n) operating at nominal power under nominal voltage and frequency, depends on the slip and the synchronous speed. Therefore, the nominal speed in rpm is calculated by:

$$n_{rpm} = n_s \cdot \left(1 - \frac{S}{100}\right) \tag{4}$$

3.2. Typical Engine Failures

The presence of a fault, even if incipient, can have a significant impact on the machine's performance, resulting in losses to the production process. Unscheduled downtime represents major challenges in the industrial sector, increasing maintenance costs and production losses. The monitoring and diagnosis of a three-phase induction machine (TIM) is based on information extracted from the equipment. This information is properly processed to ensure that its characteristics allow for a reliable analysis [22]. The ongoing search for optimizing efficiency and productivity extends beyond merely adopting new technologies to replace manual work. Today, it also involves generating and analyzing large amounts of data related to the maintenance and operating conditions of production line components [24]. A fault detection and diagnosis system can be a crucial tool for the maintenance sector in various industries. One of its main advantages is the ability to identify failures at early stages, which not only facilitates the implementation of predictive maintenance but can also prevent unscheduled machine downtime.

Figure 2 shows the fault-classification tree in a TIM divided into two classes: electrical faults and mechanical faults. The percentages of failures in three-phase induction motors can be distributed as follows: bearing-related failures: 40%, stator winding failures: 38%, rotor-related failures: 10%, other failures: 10% [4].

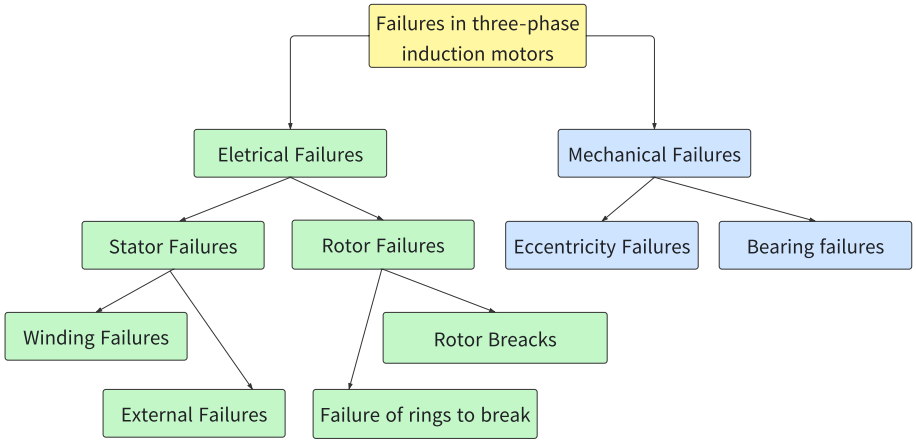

Figure 2. Failure tree.

3.3. AI Techniques Applied to Engine Fault Detection

One of the most interesting topics in the field of science is the concept of intelligence. Since the dawn of civilization, both philosophical thinkers and scientists have dedicated themselves to understanding the intelligence of nature and how it manifests itself in living organisms. With technological advances, especially with the introduction of digital

computing systems in the 20th century, questions arose about the possibility of computers being capable of demonstrating behaviors that could be considered intelligent [25].

The implementation of artificial intelligence techniques in fault detection allows real-time monitoring to be carried out using computers, requiring minimal interaction with the user. In several situations, these technologies are capable of diagnosing faults without the need for intervention from maintenance specialists [26].

Condition monitoring in induction motors is a process divided into several phases. This includes information collection, predictive analysis, feature extraction, and fault identification using machine learning (ML) algorithms. To develop a classifier with ML algorithms, intelligence-based fault-identification systems must undergo data extraction algorithms. Several strategies are employed for function identification and classification, including evolutionary algorithms, angular improvement, and data extraction. Machine learning algorithms, such as k-nearest neighbors, Artificial Neural Networks, support vector machines, random forests, Bayesian classification algorithms, Naïve Bayes, and intelligent systems, have been successfully used to build intelligence methods. Recently, researchers have been exploring supervised learning for fault identification [27].

Artificial Neural Networks (ANNs) represent a powerful tool for the accurate diagnosis of faults in induction motors (IMs). These networks are effective pattern classifiers, which makes them capable of solving a wide range of problems, especially those that involve the recognition of variables that cannot be fully described or predicted, as is the case with failures in MIs. Thus, by creating a neural network, we can successfully address pattern classification issues, which proves to be fundamental in the detection and accurate diagnosis of faults in induction motors [28].

3.4. Recurrent Neural Networks

Recurrent neural networks (RNNs) are characterized by their ability to retain information by feeding back the outputs of one or more neurons. This mechanism allows recurrent networks to maintain internal states that evolve dynamically, incorporating both new inputs and weights from previous states. This characteristic gives RNNs a structure that resembles a memory, where relevant information is preserved and used for subsequent processing. A dynamic neural network can be characterized as one that contains synaptic feedback connections between layers and delays that enable the transmission of the dynamics of a phenomenon through neurons from different layers, as illustrated in Figure 3. In this way, recurrence can be defined as a type of short-term memory, which allows for the network process of retrieving information from the recent past.

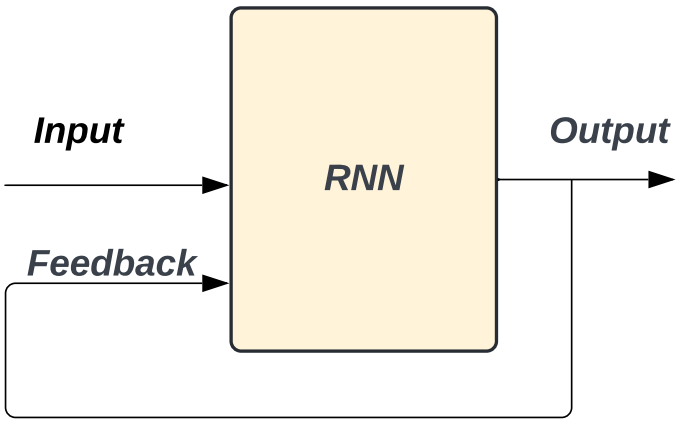

Figure 3. Topology of a recurrent neural network.

The NARX model is a form of recurrent Artificial Neural Network with feedback mechanisms, especially suitable for the nonlinear modeling of systems, focusing on time series, where past data are used to predict future values [29]. NARX networks are an efficient alternative to recurrent networks, offering similar computational efficiency. The

NARX model integrates both the initial input data and the output data generated after training. In this way, the network can improve its capacity for continuous learning [30].

Figure 4 shows the topology of a NARX neural network, where u represents the external input, y denotes the previous response, and $y(k)$ is the estimated output. The blue boxes indicate the network's delays, while the numbered circles represent the neurons in the hidden layer.

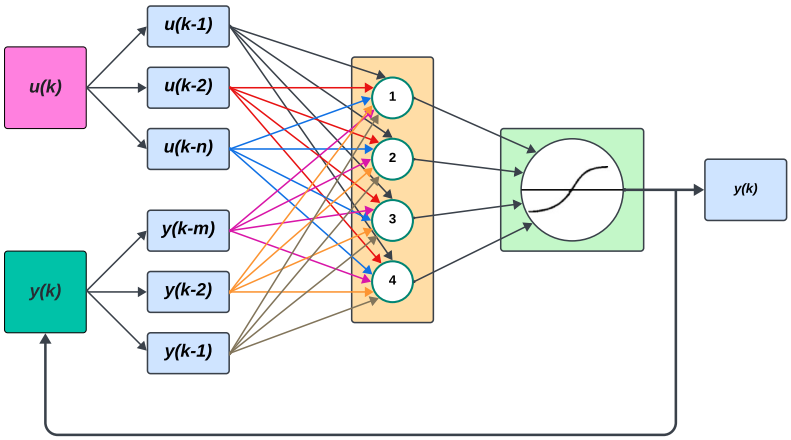

Figure 4. Topology of a NARX neural network.

The equation that defines the NARX model is

$$y(k) = f(u(k-1), u(k-n), \ldots, y(k-m), y(k-1)) \quad (5)$$

where
u_k—the input feature vector for the network.
y_k—the output vector for the network.
n—the index of the nth coefficient in $u(k)$.
m—the index of the nth coefficient in $y(k)$.

3.5. Evaluation Metrics for Classification in Machine Learning

The machine-performance-evaluation learning algorithm on a specific dataset is carried out by measuring how well the predictions generated by the adjusted model reflect the observed values for the variable of interest.

Classification is based on predicting the category of a given observation. Some of the applications of ANNs are related to pattern classification. In these applications, the neural network is trained to distinguish an unknown pattern among several classes or categories. Thus, when faced with an unknown pattern, the neural network must assign it to one of the existing classes. To evaluate the classifier's performance with new patterns (patterns different from those used in training), it is necessary to carry out a testing or practical application phase. During this phase, we evaluate the number of hits made by the classifier on a set of patterns whose classes are known. It is important to highlight that none of the patterns in this set must have been used during the training of the classifier [31].

3.5.1. Predicted Data Classes: TP, TN, FP, and FN

In a classification problem, there are two possible solutions: right or wrong. However, for a binary classification problem, there are still two other possible classes that are called positive and negative classes.

True positive (TP): when the method says that the class is positive and, when checking the answer, it can be seen that the class was positive.

True negative (TN): when the method says the class is negative and, when checking the answer, it is seen that the class was negative.

False positive (FP): when the method says that the class is positive, but instead when you check the answer, you see that the class was negative.

False negative (FN): when the method says that the class is negative, but when checking the answer, it is seen that the class was positive.

3.5.2. Evaluation Metrics

In contexts where the number of classes exceeds the binary paradigm, the complexity of the problem increases, making it prone to mistakes in the implementation of multiclass classifiers. Therefore, several parameters are used to evaluate the effectiveness of a classifier in artificial intelligence systems [32].

The main metrics that can be used to evaluate the quality of a classifier are the following:

Accuracy: The proportion of correct predictions about the total number of predictions. The accuracy metric is commonly used as one of the main criteria in the evaluation of classifiers in artificial intelligence. This is due to its effectiveness and its conceptually simple nature, which facilitates its understanding [32]:

$$\text{Accuracy} = \frac{\text{Correct predictions}}{\text{Total predictions}} \tag{6}$$

Precision: Calculates the proportion of true positives about all examples classified as positive. Precision seeks to answer the following question: what percentage of predicted true positives is correct? It represents the proportion of true positives in all classified positive values (true positives plus false positives). When the number of false positives is high, accuracy decreases significantly. It is generally used when false positives have a potentially more harmful impact than false negatives [32]:

$$\text{Precision} = \frac{TP}{TP + FP} \tag{7}$$

Recall: Also referred to as recall or "sensitivity", this metric seeks to answer the following question: what percentage of all true positives were predicted correctly? It is calculated as the ratio of true positives to the sum of true positives and false negatives. This metric is commonly applied in situations where false negatives are potentially more concerning than false positives. It evaluates the rate of true positives that the model can predict, allowing for an analysis of the classifier's ability to identify false negatives [32]:

$$\text{Recall:} = \frac{TP}{TP + FN} \tag{8}$$

F1 score: The score (or simply F1-Score for true values) combines two essential metrics in binary machine learning classifiers: accuracy and recall. It is calculated as the harmonic mean of these metrics. A low F1 score indicates that both precision and recall are below optimal levels, suggesting the need for adjustments in the classifier. The F1 score is a machine learning model performance metric that assigns equal weight to accuracy and recall. The results provided by this metric offer high-level, reliable insights into the classifier' output [32]:

$$\text{F1} - \text{Score} = 2 \cdot \frac{\text{Accuracy} \cdot \text{Recall}}{\text{Precision} + \text{Recall}} \tag{9}$$

ROC Curve: Within the analysis of the performance of classification models, there are a variety of statistical estimators used. One of the most common is the ROC curve (Receiver Operating Characteristic), which offers a graphical representation of a model's performance in relation to its sensitivity (the fraction of true positives) and its specificity (the fraction of false positives) at different cutoff points. On the X-axis (horizontal), we have the false positive rate (Specificity: $1 -$ specificity), and on the Y-axis (vertical), we have the true positive rate (sensitivity). The Figure 5 show examples of ROC curves represented in green, orange, and blue. The closer the sensitivity and specificity values are to 100%, the

higher the accuracy of the test. The ROC curve demonstrates how sensitivity and specificity vary as different cutoff values are considered [33].

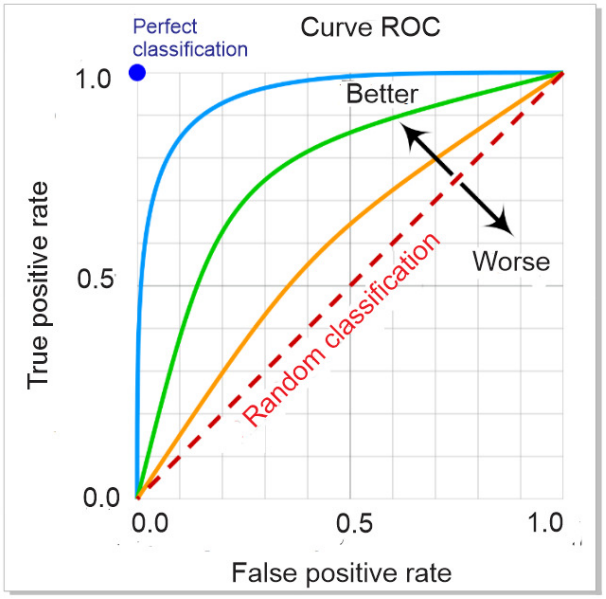

Figure 5. ROC curve.

Confusion matrix: The confusion matrix is a technique widely used in evaluating classification algorithms. Also referred to as an error matrix, it consists of a table that simplifies the analysis of the performance of such algorithms. The data contained in this matrix are essential for the mathematical formulation of various classification metrics. It is made up of the number of true positives (TPs), true negatives (TNs), false positives (FPs), and false negatives (FNs).

$$\text{Accuracy} = \frac{TP + TN}{TP + FN + TN + FP} \tag{10}$$

The multiclass confusion matrix illustrated in Figure 6 can be interpreted as follows: the main diagonal, colored green, represents the true positives (TPs); above the main diagonal are the false positives (FPs); and below the main diagonal are the false negatives (FNs).

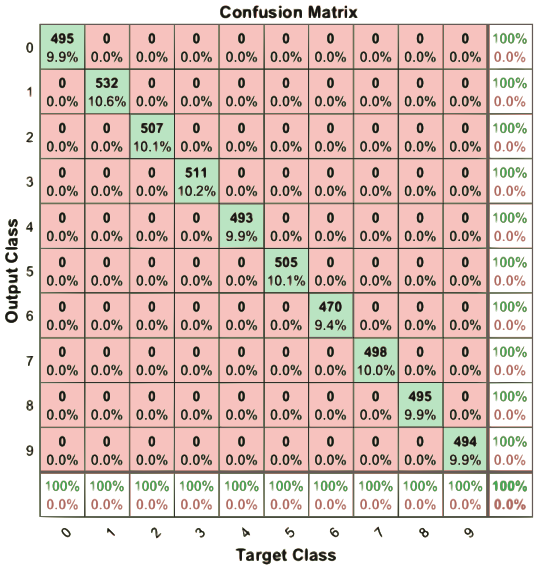

Figure 6. Confusion matrix for multiclass classification.

3.6. Remarks

The good performance of the three-phase induction motor is due to its simple and efficient construction. Due to this simplicity, associated with robustness and low cost, the three-phase induction motor is placed on the list of the most used motors in industries.

The cost of equipment maintenance is still considerably high in the industry. Therefore, developing systems that enable the monitoring and diagnosis of possible failures can reduce this cost. To develop these systems, various techniques have emerged.

One of the most used techniques has been artificial intelligence. This technique has been very important for solving complex problems. Artificial intelligence makes it possible to detect faults that may occur in the three-phase induction motor more quickly and accurately. Two important areas of artificial intelligence are presented: machine learning and deep learning.

There are several evaluation metrics commonly used in machine learning, each with its specific purpose and interpretation. Choosing the appropriate metrics depends on the type of problem we are addressing and the objectives of the model.

4. Materials and Methods

This section covers a detailed description of the methodology adopted in the development of the monitoring and fault-diagnosis system for three-phase induction motors. The experiments were carried out on an experimental bench installed in the machine laboratory of the Federal University of Rio Grande do Norte (UFRN). The experimental bench used in this research emulates a real engine operation application. Two categories of failures were diagnosed: mechanical failures (unbalanced shaft and defective bearings), which are identified through vibration and temperature analysis, and electrical failure (defective stator), identified through winding current and temperature signals. These current, vibration, and temperature signals were used to build a dataset to feed the input to the NARX neural network. The tests were conducted under normal operating conditions, as well as in simulated failure situations, including stator voltage unbalance, shaft unbalance, and bearing defects. The subsequent sections aim to detail the procedures, materials, and methods used in signal acquisition, as well as explain how the faults were emulated.

Figure 7 show the block diagram used to implement the proposed methodology. The diagram is organized into five main blocks. Block 1 corresponds to the test bench, where faults will be simulated in the installed motor. Block 2 is responsible for data collection, performed through the reading of signals captured by vibration, current, and temperature sensors. In Block 3, the collected signals are processed using LabVIEW software, where both time-domain and frequency-domain graphs are generated. Block 4 performs fault classification using the NARX neural network. Finally, in Block 5, the classified fault results are presented.

The subsequent sections aim to detail the procedures, materials, and methods used in the signal acquisition, as well as explain how the faults were identified.

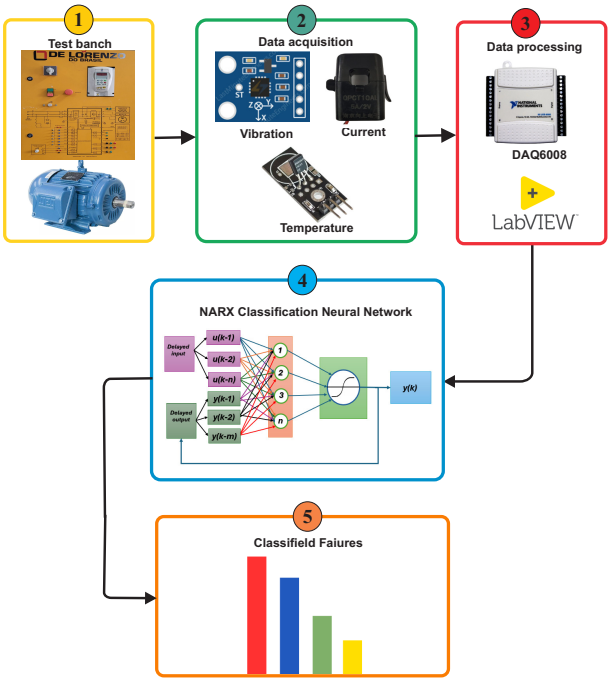

Figure 7. Process flowchart.

4.1. Materials—Test Bench

The bench used to carry out the experiments is the DLB MAQ-RN, manufactured by the company De Lorenzo of Brazil. This bench is equipped with the necessary resources for the execution of signal acquisition procedures and the identification of faults in an efficient and precise manner, enabling reliability in results and consisting of a WEG of Brazil brand frequency inverter model CFW-09 with power 1.5 CV and current 10A and a cage-type induction motor.

Figure 8 shows the complete bench, Figure 9 shows the three-phase induction motor, and Table 1 shows the characteristics of the motor.

Figure 8. Test bench.

Figure 9. Three-phase induction motor.

Table 1. Characteristics of the three-phase induction motor.

Features	Data
Power	1.1 HP
Speed	1720 RPM
Frequency	60 Hz
FS	1.5
Ip/In	7.8 A
Voltage	220/380 V
Current	4.43/2.56 A

4.2. Materials—Data Collection

Data collection was carried out using five sensors, strategically installed in the engine. These include three current sensors distributed across the three phases that power the motor, providing a comprehensive analysis of its electrical performance. Furthermore, a temperature sensor was positioned to monitor thermal variations, while an accelerometer-type vibration sensor was used to evaluate the mechanical oscillations of the system. This variety of sensors allows for comprehensive data collection, offering valuable insights into many aspects of engine operation.

4.2.1. Current Measurement

To measure three-phase currents in the stator, noninvasive current sensors based on the Hall effect were used, specifically the 5A/2V model - OPCT 10AL.

Figure 10 shows the noninvasive current sensor, and Table 2 shows its characteristics.

Figure 10. Current sensor.

Table 2. Characteristics of the current sensor.

Features	Technical Data
Rated Input	5 A (AC)
Rated Output	5 V (DC)
Accuracy error	0.5%
Linearity	0.5%

Converting AC Voltage Signal to DC

The sensor was calibrated to measure the maximum alternating current of 5A AC. This 5A value is the RMS value, which is also called the effective value. The RMS value is equal to the maximum value that the current can reach (peak current) divided by the square root of two. At the sensor output, the induced current signal is similar to that in Figure 11.

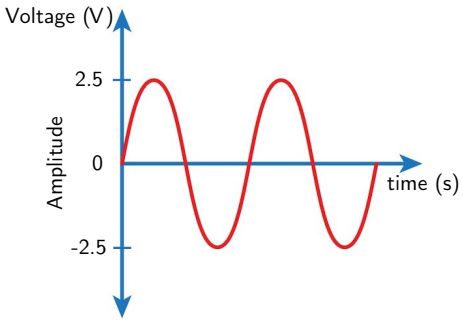

Figure 11. Signal at the output of the sensor.

In Figure 11, an alternating voltage signal oscillating between positive 2.5 V and negative 2.5 V is shown. However, the DAQ-6008 interface device, being powered by a, is capable of measuring signals within the range of 0 to 5 V. Therefore, it is necessary to adjust the signal so that the signal variation is in the range of 0 V to 5 V. To achieve this adjustment, initially, a voltage divider was implemented using the 5 V power supply provided by the DAQ-6008 device. In this context, we chose to configure resistors R1 and R2 with the same value, both 10 kΩ.

Figure 12 shows the signal conditioning circuit, and Figure 13 shows the conditioning board.

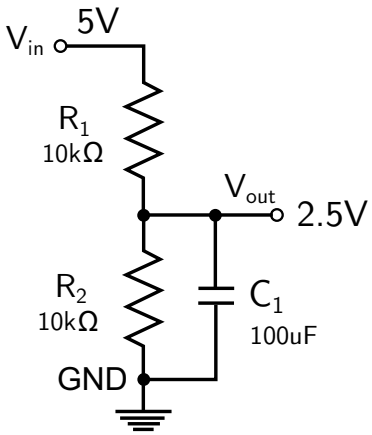

Figure 12. Current conditioning circuit.

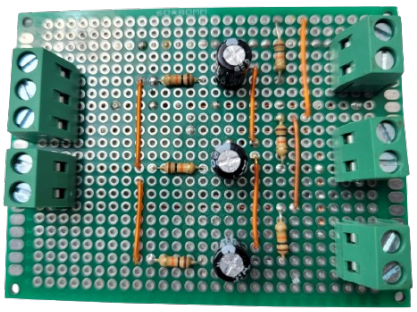

Figure 13. Current conditioning board.

This choice guarantees that the voltage across them is equal, as the 5 V coming from the device will be distributed evenly between them, as can be seen in Figure 14.

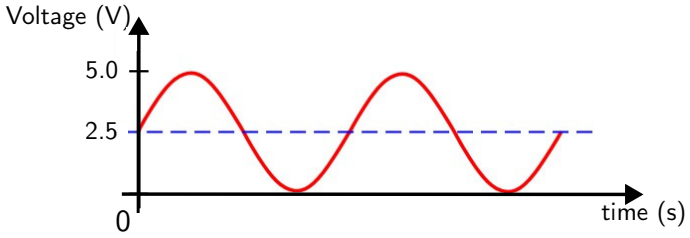

Figure 14. Sinusoidal waveform with offset value.

4.2.2. Vibration Sensor

The GY-61 DXL335 3-axis accelerometer module is an advanced sensor that utilizes the ADXL335 integrated circuit. This triaxial accelerometer offers an exceptional performance, characterized by a very low level of noise and energy consumption. With a full detection range of ±3 g, the sensor is capable of measuring both static accelerations due to gravity, in tilt sensing applications, and dynamic acceleration resulting from movement, impact, or vibration.

Figure 15 shows the vibration sensor, and Table 3 shows the characteristics.

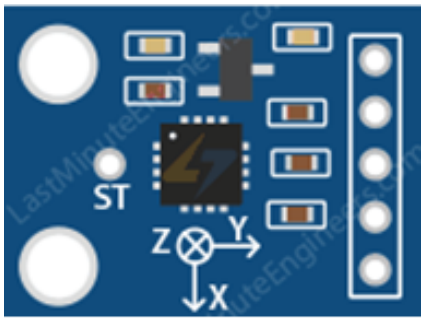

Figure 15. Vibration accelerometer sensor.

Table 3. Characteristics of the vibration sensor.

Features	Technical Data
Sensor Chip	ADLX335
Operating voltage range	3 to 5 V (DC)
Supply current	400 µA
Scale range	±3 g
Operating temperature	−40 °C to +85 °C
Sensitivity	300 mV/g
Accuracy	±10%

4.2.3. Temperature Measurement

To measure the engine temperature, the LM35DZ temperature sensor module was used. The LM35DZ temperature sensor consists of a high-precision integrated circuit, whose output voltage varies linearly about the temperature in degrees Celsius. The LM35DZ device eliminates the need for external calibration or adjustments, providing remarkable accuracies of $\pm\frac{1}{4}$ °C at room temperature and $\pm\frac{1}{4}$ °C over a wide thermal range, ranging from −55 °C to 150 °C.

Figure 16 shows the temperature sensor module, and Table 4 shows its characteristics.

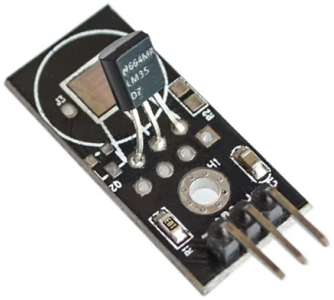

Figure 16. Temperature sensor.

Table 4. Characteristics of the temperature sensor.

Features	Technical Data
Operating voltage	4 to 30 V
Drain current	<60 µA
Measuring range	−55 to 150 °C
Sensitivity	10 mV/°C
Accuracy	0.5 °C (at 25 °C)

4.3. Data Processing

During the data collection stage, the sensors were connected to the DAQ—USB-6008 interface board, manufactured by National Instruments, to capture the signals, which were later read in the LabVIEW software. ADAQ—USB-6008 is an affordable and user-friendly solution for interfacing input and output signals with a personal computer. Connectable via a simple USB cable, this board offers a direct and efficient connection to the PC.

Figure 17 shows the voltage sensor module, and Table 5 shows its characteristics.

Figure 17. NI USB 6008.

Table 5. Characteristics of the NI USB-6008.

Features	Technical Data
Supply voltage	5VDC
Analog inputs 12/14 bits	8
Analog outputs 12 bits	2
32-bit	5 Mhz counter
Sampling Rate	1 KHz
Acquisition Mode	Continuous Samples
Recommended Software	LabVIEW

LabVIEW Block Diagram Code

Programming on the LabVIEW platform was carried out through a graphical interface in the block diagram, where each block represents a specific LabVIEW function. In the case of the vibration-, current-, voltage-, and temperature-monitoring program, the analyses are

continuous, and therefore it is necessary to implement a loop (while) to execute in cycles. This loop is interrupted when a stop condition is reached, such as pressing the stop button.

The graphs are generated according to the selected quantity. In this process, the graphics block identifies one of the signals given in its input and applies a Fast Fourier Transform (FFT) to the signal. Subsequently, the data are presented in both the time and frequency domains, allowing for visualization in the corresponding graphs. In addition to the graphical representation, the data are exported to Excel, where they are compiled into a database. This database is essential to feed the artificial intelligence algorithms used later.

Figure 18 shows the block diagram developed in LabVIEW software to perform signal processing. The diagram is divided into five blocks: block 1, DAQ assistant, is responsible for configuring the ports on the data acquisition board; block 2 is responsible for configuring the reading of the vibration signal for the three axes of the accelerometer and generating graphs to display these signals in both time and frequency; block 3 has the same function as block 2, but for the current signal, generating similar graphs; block 4 is responsible for configuring the temperature signal reading and displaying this signal through a graph; and in block 5, the while loop time and the determination of the stopping criteria are configured.

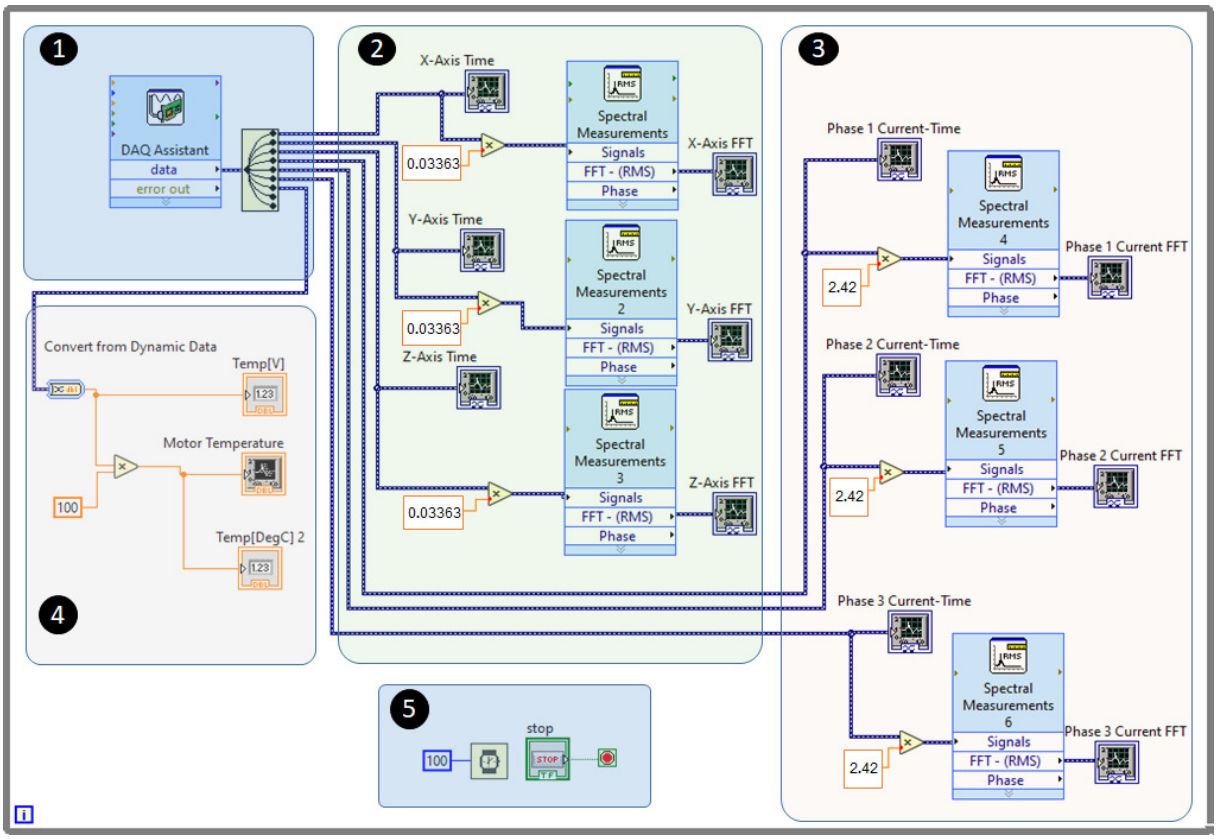

Figure 18. LabVIEW block diagram.

4.4. Methodology of the Fault-Detection Process

This section describes the methodology adopted to build the database from the signals collected in the engine, as well as the process of normalizing these data and the development of the fault-classification algorithms addressed in this work.

For training, validation, and testing of the neural network, a set of data was constructed from the signals collected by the sensors installed in the engine, having a csv table format with columns referring to the network's input and output data. The dataset, in turn, was subdivided into three sets, one for training, another for validation, and another for testing, following the proportions 70%, 15%, and 15%, respectively.

After creating the datasets, they were normalized. Normalization is a process by which data are adjusted to a scale with a range between zero and one. This practice is crucial, as neural network models tend to perform optimally when inputs are in this range. Equation (11) shows the formula used to calculate the normalized value of input X:

$$\mathbf{X}_{standardized.} = \frac{X - X_{min}}{X_{max} - X_{min}} \tag{11}$$

NARX Neural Network for Classification

The NARX (Nonlinear AutoRegressive with Exogenous inputs) neural network is a powerful architecture for modeling nonlinear dynamical systems, enabling accurate predictions and adaptation to changing operating conditions. This work explores significant modifications to network parameters, such as the cross-entropy loss function and the use of the softmax activation function at the output, specifically aimed at diagnosing faults in three-phase induction motors.

Changes in the parameters of the NARX neural network open up significant opportunities for its application in categorical multiclass fault-classification tasks. Although the original NARX framework is widely used for time series forecasting and modeling, these modifications allow it to be adapted for classification problems, especially where temporal characteristics are essential for identifying fault patterns and characteristics.

One of the main advantages of this approach is the ability to use the architecture of neural networks to extract and learn complex representations of input data, including past temporal information. With modifications to the parameters, the network can focus on identifying patterns and characteristics relevant to classifying faults.

Furthermore, adopting a NARX network for categorical multiclass classification enables the use of specific evaluation techniques and metrics for classification problems, such as precision, recall, F1 score, and confusion matrix. This allows for a more accurate assessment of network performance in identifying and classifying different types of faults.

Another significant advantage is the flexibility of this approach. By using a modified neural network structure, it is possible to easily tune the network architecture, experiment with different configurations of hidden layers, activation functions, and training methods, optimizing the network performance for the specific fault-classification problem.

In summary, when using a NARX network in the categorical multiclass classification of faults, benefits such as the ability to extract relevant temporal information, the use of specific classification techniques, and the flexibility to adjust the network architecture are obtained, better meeting the needs of the problem in question.

Figure 19 shows the topology of the NARX neural network for categorical multiclass classification.

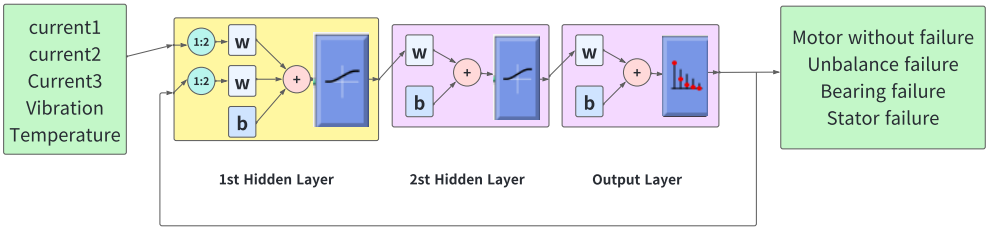

Figure 19. NARX neural network.

5. Results

Next, the results obtained from the proposed methodology application will be presented, which aim to evaluate the performance of the NARX neural network through comparisons of dynamic response and efficiency. These results were obtained through tests conducted on the experimental bench in the Automation and Control Laboratory of the Federal University of Rio Grande do Norte. Four scenarios were established for data

collection, which will be described below. Then, the NARX neural network will be trained, validated, and tested based on this collected data.

5.1. Scenarios for Data Collection

The programmed failure test followed a script with the development of five scenarios for case studies, aiming to identify failures in the electric motor through signal analysis. The scenarios were developed to represent various engine operating conditions, including normal operating situations and simulated failures, such as shaft unbalance, bearing damage, and stator current unbalance. The tests were carried out at three speeds: 900 RPM, 1200 RPM, and 1800 RPM. For this article, only data for the 1800 RPM speed are presented.

5.1.1. Scenario 1: Collecting Data from the Engine in Good Operating Conditions

This scenario serves as a reference point, representing normal engine operation under ideal conditions. Vibration, electrical current in the phases, and temperature signals were collected. Figure 20 shows the engine with the sensors installed. Figures 21 and 22, respectively, show the signals in the time domain for vibration and current signals, while Figures 23 and 24 illustrate the signals in the frequency for the same signals. Figure 25 shows the temperature in ideal engine conditions.

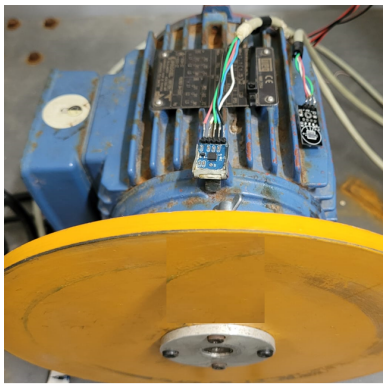

Figure 20. Sensors installed in the motor.

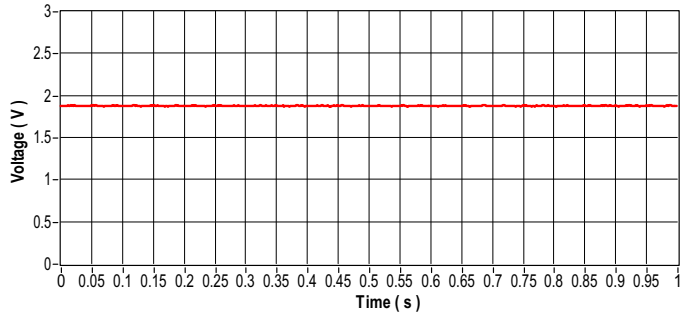

Figure 21. Vibration signal in the time domain.

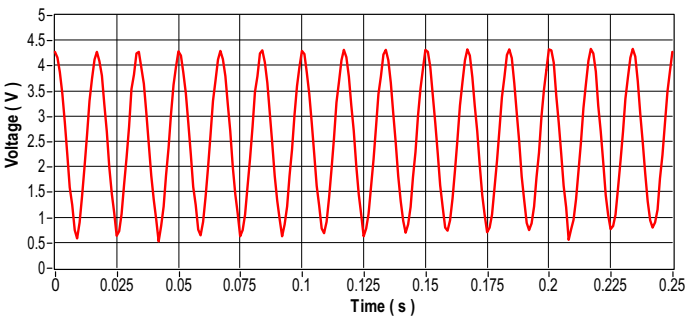

Figure 22. Current signal in the time domain.

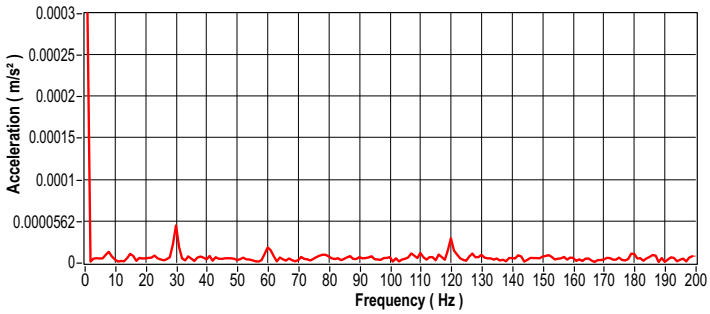

Figure 23. Vibration signal in the frequency domain.

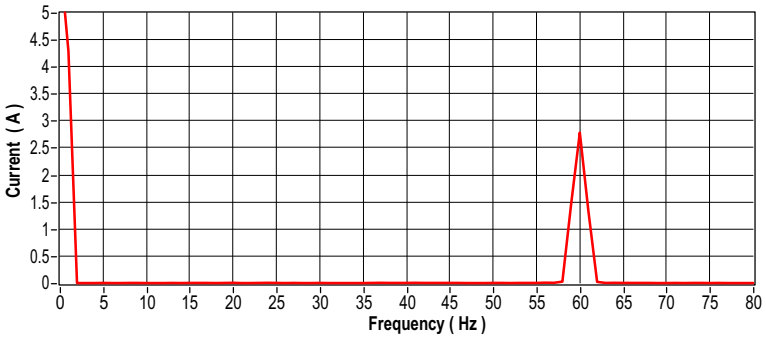

Figure 24. Current signal in the frequency domain.

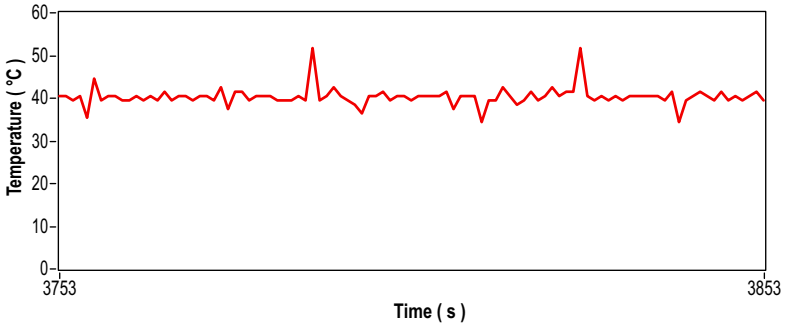

Figure 25. Signal of motor temperature under good operating conditions.

5.1.2. Scenario 2: Motor Data Collection with Shaft Unbalance

Engine unbalance is characterized by the uneven distribution of mass around the axis of rotation of the engine shaft. Due to this imbalance, the centripetal forces generated during the operation increase bearing wear. The phenomenon is typically observed in all rotating machines and is identified by an amplitude peak at the shaft rotation frequency, shown in the frequency spectrum.

To create a dynamic eccentricity that corresponds to an unbalance in the motor shaft for this scenario, a mass weighing 28 g was used. Figure 26 shows its fixation on a disc coupled to the motor shaft. The vibration signal that results from the induced unbalance is shown in Figure 27. The vibration signal for this case presents a sinusoidal pattern, as is typical of an unbalance. Figure 28 shows the frequency domain analysis, showing an amplitude peak at the shaft rotation frequency that corresponds to 30 mechanical Hz for a speed of 1800 RPM. The current signal in the time and frequency domains is shown in Figures 29 and 30, respectively, and the motor temperature variations are shown in Figure 31. These graphs provide more information about the behavior of the motor with the shaft unbalanced. Comparing the current signal with the unbalanced shaft and the current signal with the motor in ideal conditions, it can be seen that the current underwent a small change, changing from 2.8 A to 3 A. The temperature remained within the same variation range.

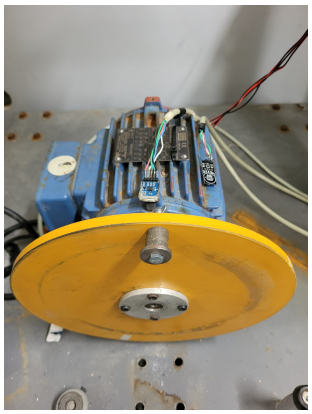

Figure 26. Installation of mass for unbalancing.

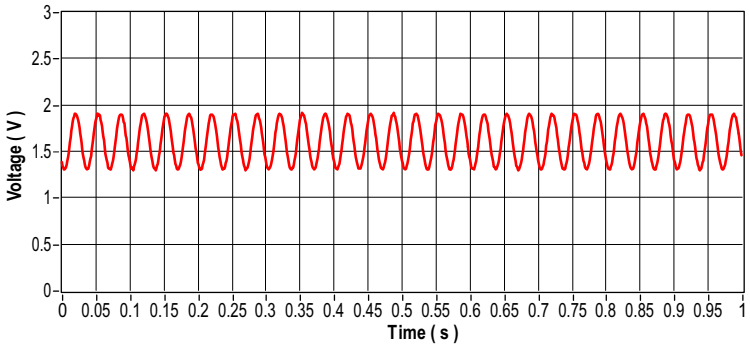

Figure 27. Vibration signal in the time domain.

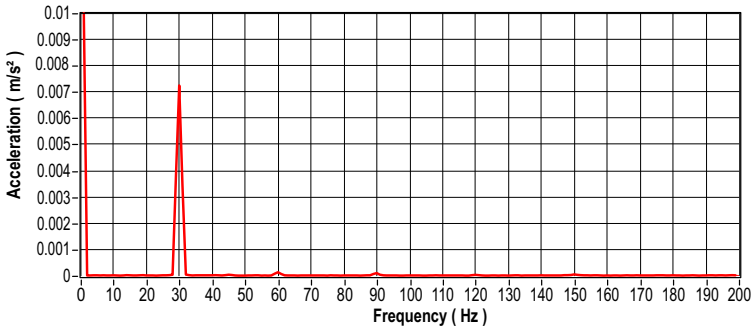

Figure 28. Vibration signal in the frequency domain.

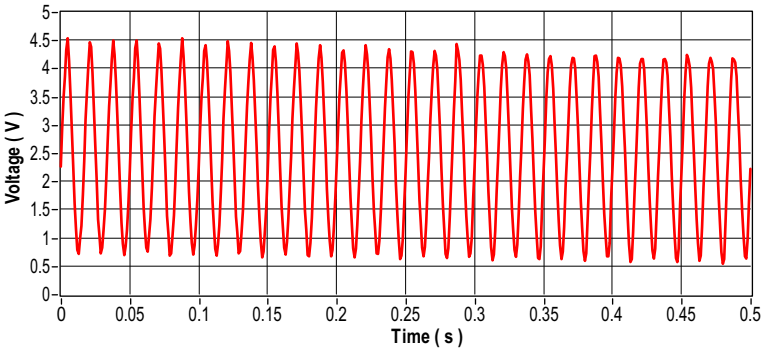

Figure 29. Current signal in the time domain.

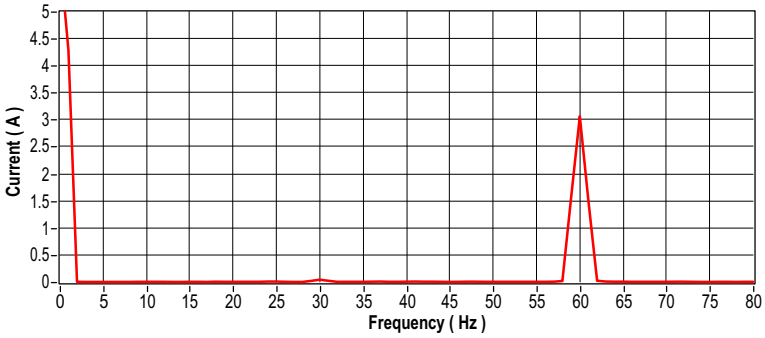

Figure 30. Current signal in the frequency domain.

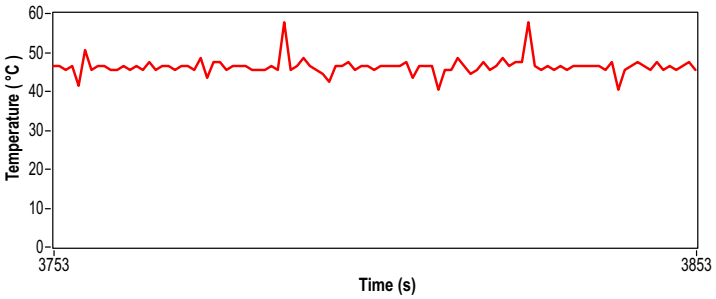

Figure 31. Temperature signal for the unbalanced motor.

5.1.3. Scenario 3: Data Collection from the Engine with Failed Bearings

Bearings consist of inner and outer rings, rolling elements (such as balls or rollers), and a cage. This component is widely recognized as one of the most frequent causes of failures in rotating machines. The premature emergence of failures is generally associated with inadequate operating conditions. Among the main factors that contribute to early bearing failures are dirt and water contamination, bearing overload, lack of lubrication, and inadequate procedures during assembly of the bearing assembly. The most common bearing failures tend to occur in the inner and outer races, and in the balls or rollers. Fault detection is usually performed by transforming the signal from the time domain to the frequency domain. This approach is adopted for several reasons. Firstly, machine faults are identified in the signal spectrum through peaks at characteristic frequencies, as each component or fault emits a unique frequency vibration. The intensity of the characteristic harmonic indicates the presence or severity of such a fault [34].

There are four basic frequencies generated by bearing defects:

- BPFI defect. Internal ring passage frequency.
- BPFO defect. Ring outer pass frequency.
- BSF defect. Rolling element passing frequency.
- FFT defect. Fundamental frequency (cage frequency).

On the SKF website, one of the main bearing manufacturers, a valuable online tool is available for calculating rotational and over-rolling frequencies. This calculator allows for the determination of bearing frequencies based on manual input of bearing geometric data. For comparison purposes with the data obtained from vibration signal analysis to identify defective bearings, calculations were carried out for the frequency of 30 mechanical Hz or 1800 RPM for the 6203–2z and 6204–2z bearings.

Figures 32 and 33 show the calculated rolling frequencies. Figure 34 shows the damaged 6403–2z and 6404–2z bearings used in this test scenario. The vibration signal is shown in Figure 35 in the time domain and Figure 36 in the frequency domain. The current signal is shown in Figure 37 in the time domain and Figure 38 in the frequency domain. The engine temperature for this scenario is illustrated in Figure 39.

Frequency Results

SKF	Rotational frequency				Frequency of over-rolling		
Designation	Inner ring	Outer ring	Rolling element set & cage	Rolling element about its axis	Point on inner ring	Point on outer ring	Rolling element
	f_i (Hz)	f_e (Hz)	f_c (Hz)	f_r (Hz)	f_{ip} (Hz)	f_{ep} (Hz)	f_{rp} (Hz)
■ 6203-2Z	30	0	11.449	59.81	148.408	91.592	119.621

Figure 32. Failure occurrence frequencies for bearings 6203–2z.

Frequency Results

SKF	Rotational frequency				Frequency of over-rolling		
Designation	Inner ring	Outer ring	Rolling element set & cage	Rolling element about its axis	Point on inner ring	Point on outer ring	Rolling element
	f_i (Hz)	f_e (Hz)	f_c (Hz)	f_r (Hz)	f_{ip} (Hz)	f_{ep} (Hz)	f_{rp} (Hz)
■ 6204-2Z	30	0	11.446	59.749	148.435	91.565	119.498

Figure 33. Failure occurrence frequencies for bearings 6204–2z.

Figure 34. Bearings with defects 6203–2z/6204–2z.

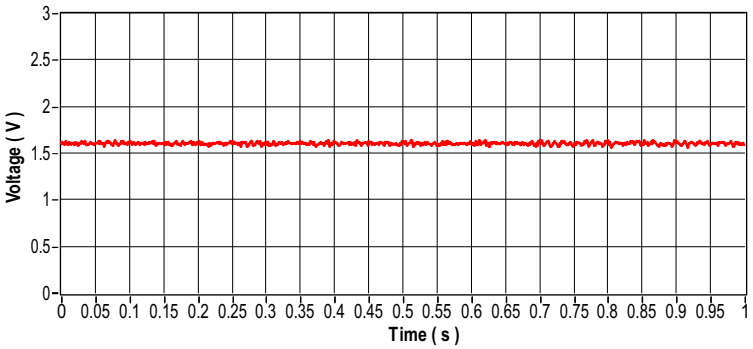

Figure 35. Vibration signal in the time domain.

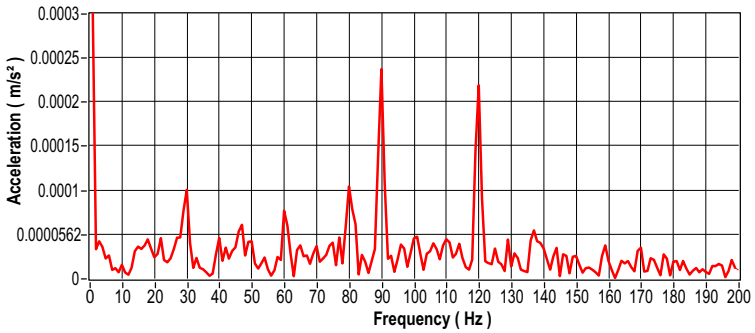

Figure 36. Vibration signal in the frequency domain.

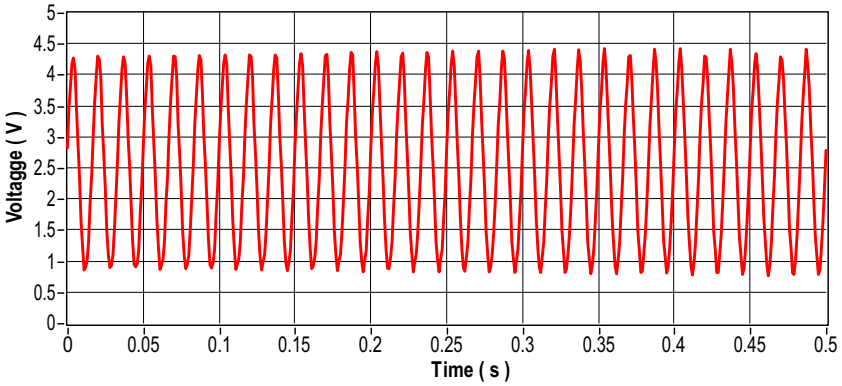

Figure 37. Current signal in the time domain.

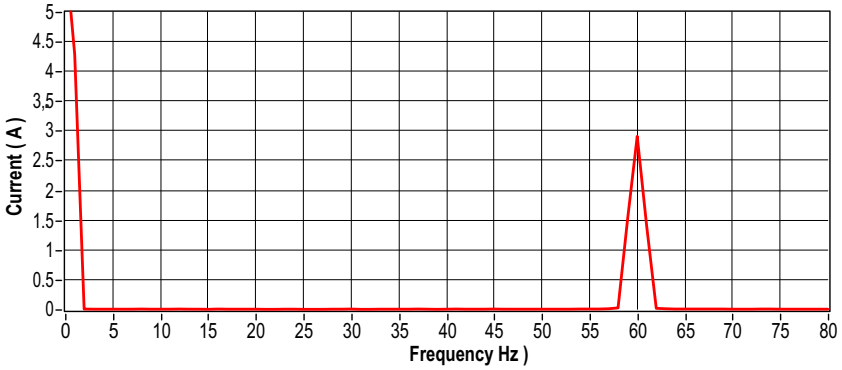

Figure 38. Current signal in the frequency domain.

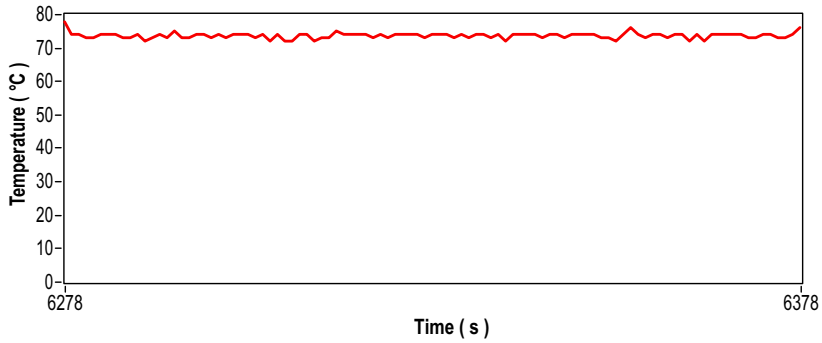

Figure 39. Temperature signal of motor bearing with defect.

5.1.4. Scenario 4: Motor Data Collection with Stator Current Imbalance

When the stator currents in an electric motor become unbalanced, several problems can arise, including overheating, excessive vibration, decreased efficiency, and premature wear. To investigate these phenomena, an approach was adopted: a bank of resistors with an ohmic load of 83.5 Ω was connected in series with one of the stator coils to cause variations in currents. Figure 40 shows the arrangement of the resistor bank used to induce such variations. Figure 41 (in the time domain) and Figure 42 (in the frequency domain) show the vibration signals recorded for this scenario. Figures 43–48 show the current readings, both in the time and frequency domains, corresponding to the three phases of the system. Finally, Figure 49 shows the temperature behavior for this same experimental scenario.

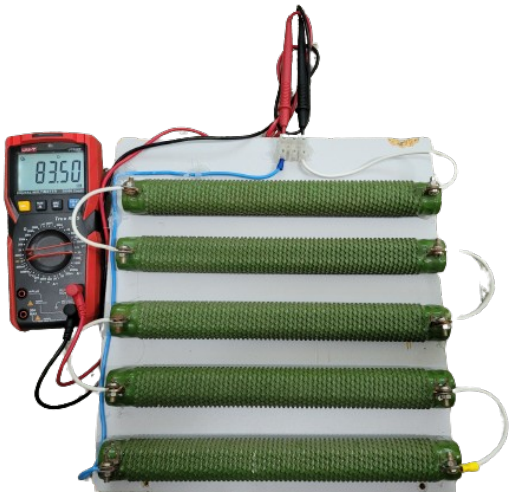

Figure 40. Bank of resistors for current unbalance.

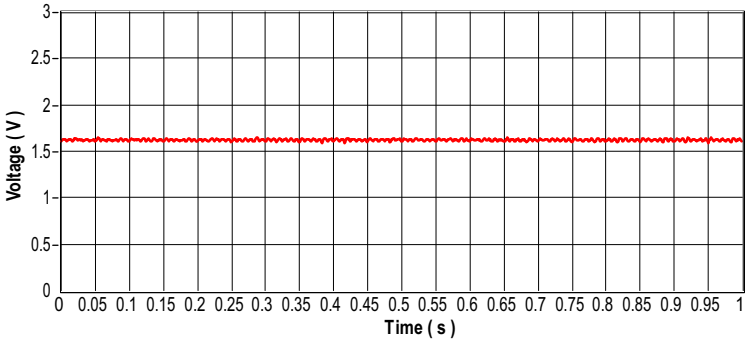

Figure 41. Vibration signal in the time domain.

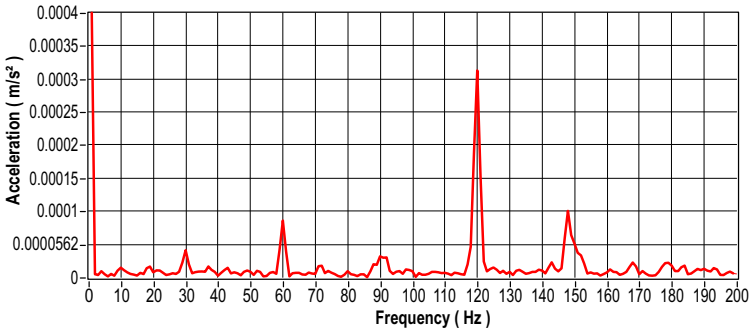

Figure 42. Vibration signal in the frequency domain.

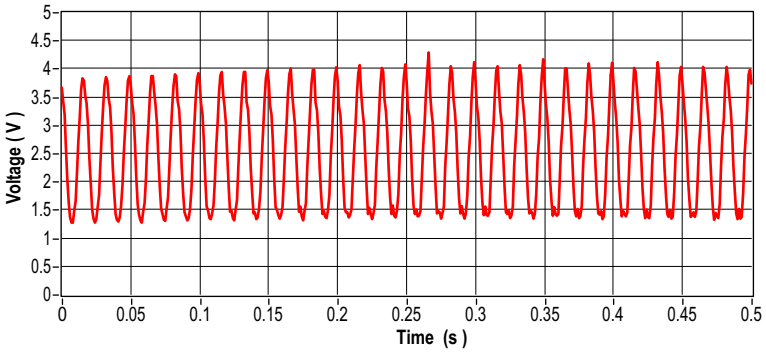

Figure 43. Current signal in the time domain—Phase 1.

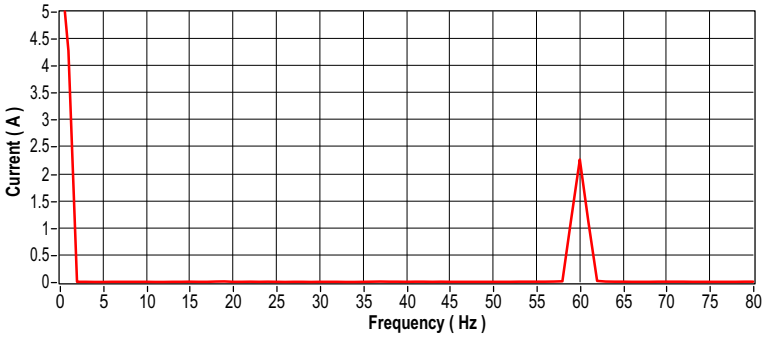

Figure 44. Current signal in the frequency domain—Phase 1.

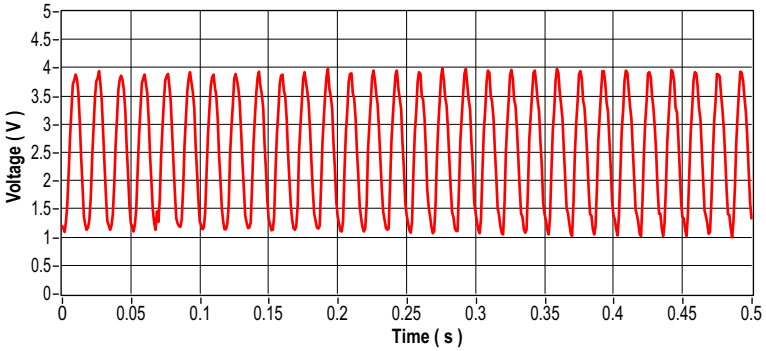

Figure 45. Current signal in the time domain—Phase 2.

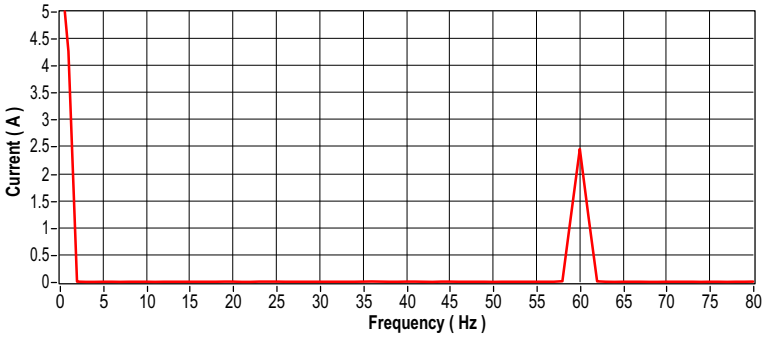

Figure 46. Current signal in the frequency domain—Phase 2.

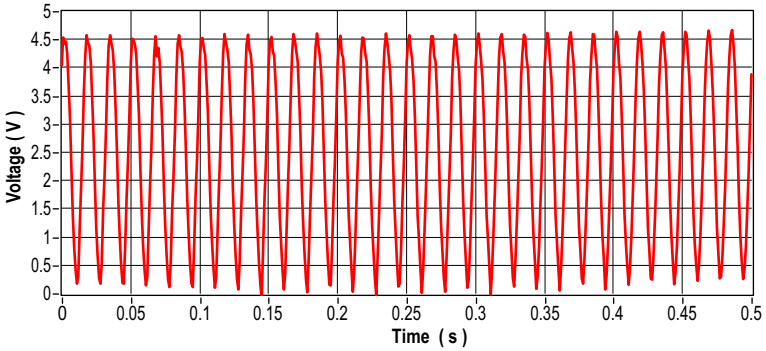

Figure 47. Current signal in the time domain—Phase 3.

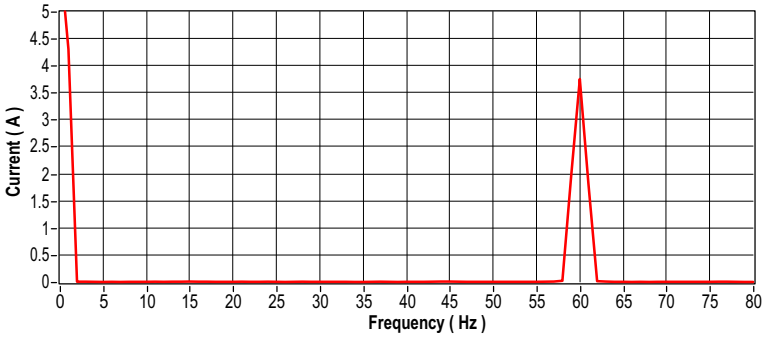

Figure 48. Current signal in the frequency domain—Phase 3.

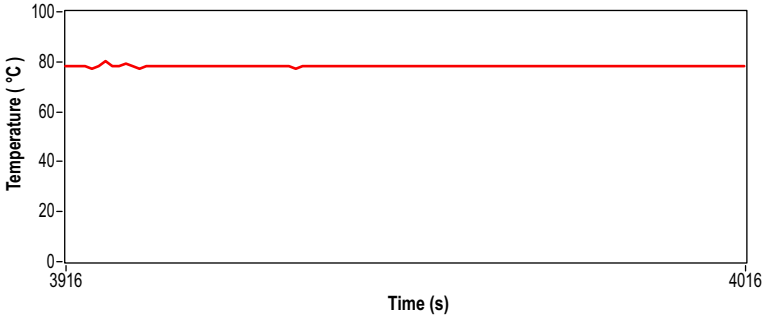

Figure 49. Temperature signal for phase unbalanced motor.

5.2. NARX Neural Network Training

The NARX network stands out for its use of recurrence and temporal delays in both inputs and feedback. During project development, it is essential to define the amount of delays and adjust other network-specific parameters, such as the number of neurons in each layer, the activation function of each neuron, and the learning algorithm used.

To obtain the best results, the NARX neural network was subjected to multiple trainings in a scan loop to determine the optimal number of neurons in the two hidden layers and the delays at both inputs and output. The training was carried out with datasets of 50 thousand events, collected from the four previously mentioned scenarios, using Matlab® software in offline mode. After training, the best network configuration was identified and subjected to testing and validation to evaluate its generalization capacity. Four different types of network outputs were examined, corresponding to different engine operating conditions: faultless motor, unbalanced defect, defective bearings, and defective stator.

During the optimization process, the following parameters were adjusted between 1 and 30 to find the optimal network configuration:

- Delay = delay steps for the input data.
- Feedback = output feedback delay steps.
- Neurons–H1 = number of neurons in the first hidden layer.
- Neurons–H2 = number of neurons in the second hidden layer.

To achieve the best network performance, the following parameter settings were determined:

- TrainFcn = 'trainscg'—"Scaled Conjugate Gradient" (SCG).
- TrainParam.epochs = 500—maximum number of training epochs.
- PerformFcn = 'crossentropy'—categorical cross-entropy cost function.
- layers1.transferFcn = 'logsig'—logistic sigmoid function first hidden layer.
- layers2.transferFcn = 'logsig'—logistic sigmoid function second hidden layer.
- layersend.transferFcn = 'softmax'—output activation function.

To train the network, a balanced dataset was used, ensuring that the number of examples of each type of failure was equal. After several training cycles, the optimal network configuration was identified, as illustrated in Table 6. Figure 50, the ROC curve,

and Figure 51, the confusion matrix, show the network's performance for the test set. Figure 52 shows the class graph showing the number of faults classified, and Table 7 presents the performance metrics of the trained network.

Table 6. Best parameters found from the trained network.

Delay	Feedback	Neurons-H1	Neurons-H2
3	4	10	10

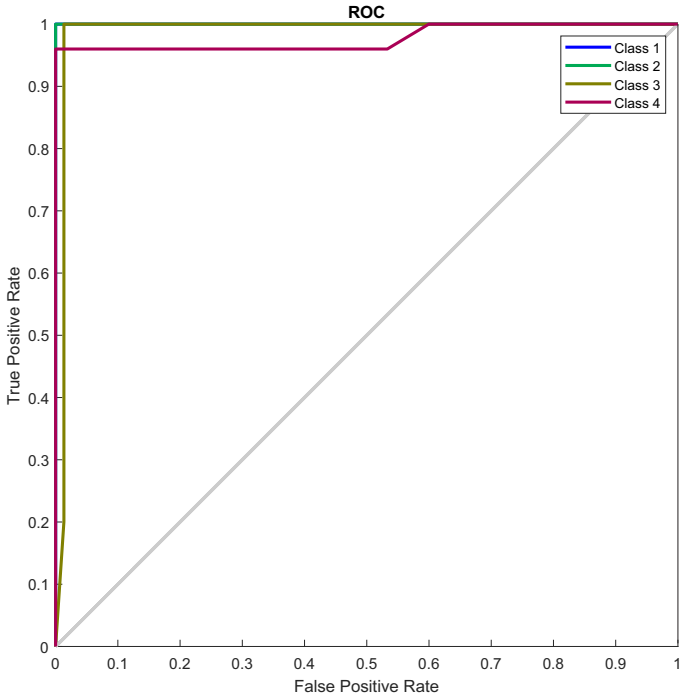

Figure 50. Standard training ROC curve.

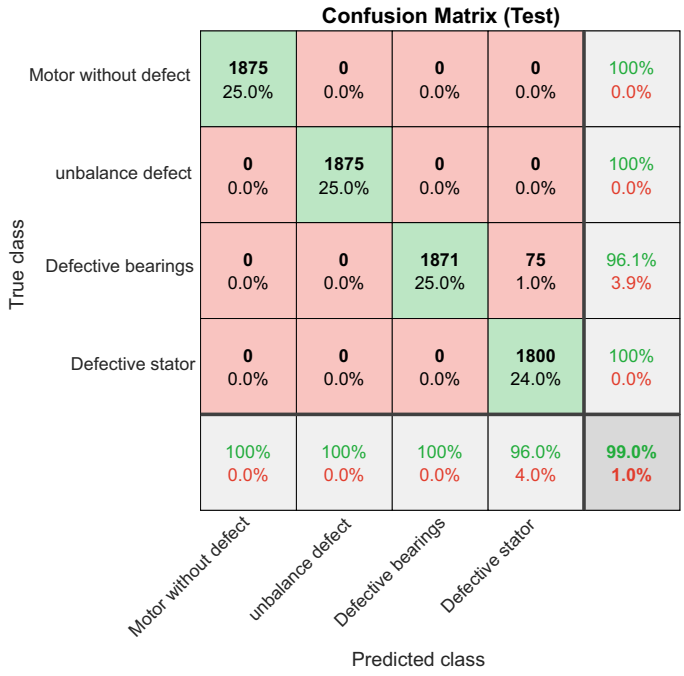

Figure 51. Standard training confusion matrix.

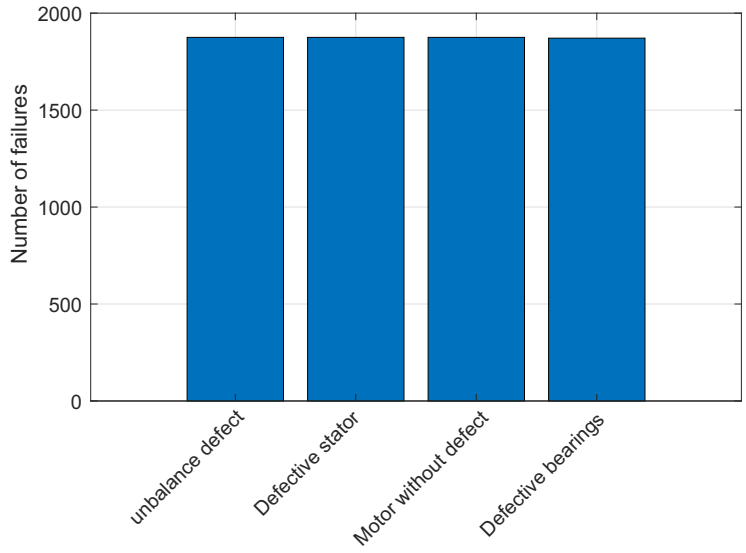

Figure 52. Failures classified in standard training.

Table 7. Performance of the trained NARX neural network.

Accuracy	Precision Total	Recall	F1 Score
0.99	1.0	0.99	0.99

Once the best network was obtained, it was necessary to validate it with new data from the engine signals. The tests described below aim to validate the NARX network implemented and trained previously to identify the four faults described in previous sections.

5.2.1. Case 1: Network Test—Motor without Failures

For this first network-validation scenario, a new dataset made up of signals collected from the engine in good operating conditions was inserted into the inputs of the NARX neural network. For this type of failure, the network responded well, achieving a performance of 94.2%. Figures 53–55 and Table 8 illustrate the network's overall performance.

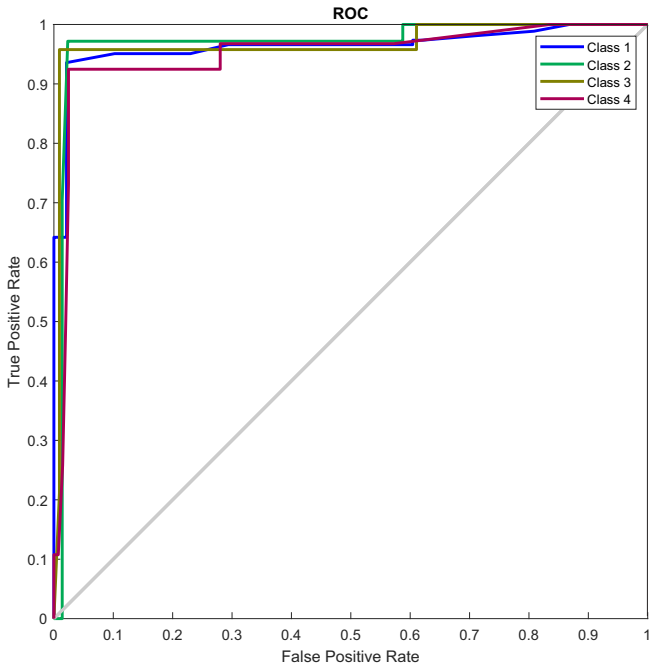

Figure 53. ROC curve of the motor without defect test set.

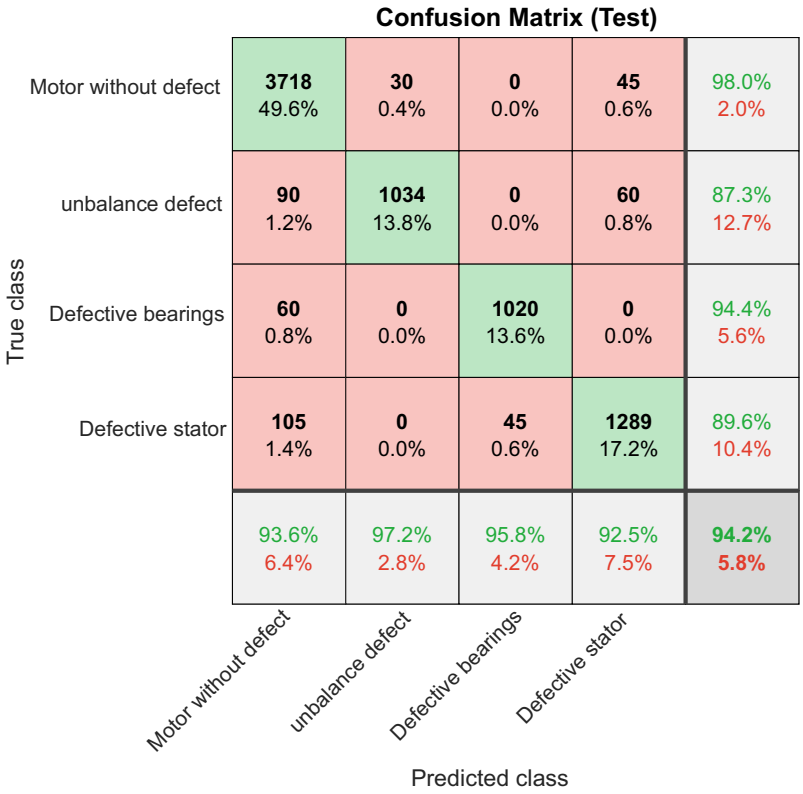

Figure 54. Confusion matrix of the 'Motor without defect' test set.

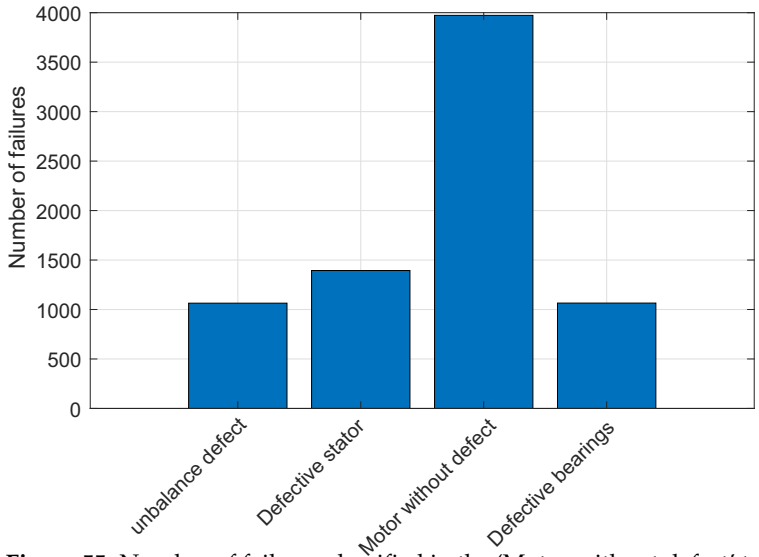

Figure 55. Number of failures classified in the 'Motor without defect' test set.

Table 8. Performance of NARX neural network for imbalance defect.

Accuracy	Precision Total	Recall	F1 Score
0.94	0.96	0.98	0.97

5.2.2. Scenario 2—Validation of the NARX Network—Unbalanced Fault

For this second network-validation scenario, a new dataset made up of signals collected from the motor with an unbalanced shaft was inserted into the inputs of the NARX neural network. For this type of fault, the network responded well, achieving a performance of 95%. Figures 56–58 and Table 9.

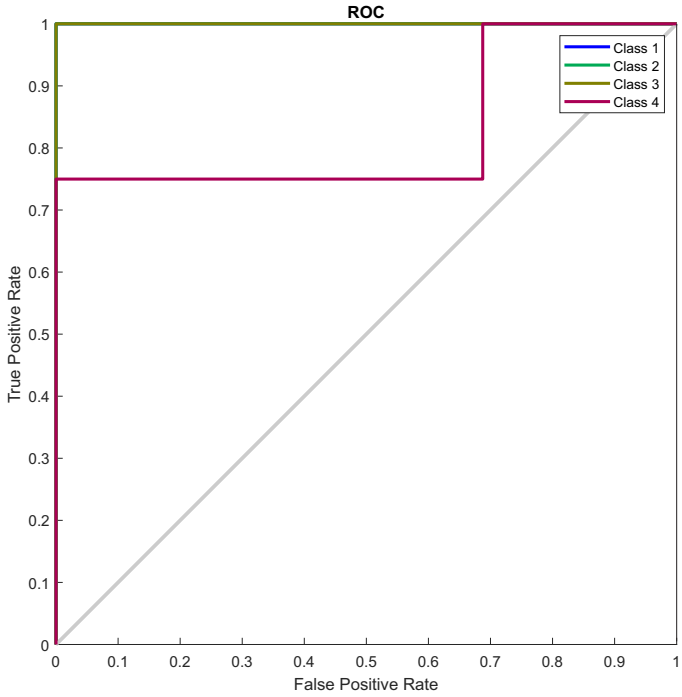

Figure 56. ROC curve of the defect unbalanced test set.

Figure 57. Confusion matrix of the 'Defect unbalance' test set.

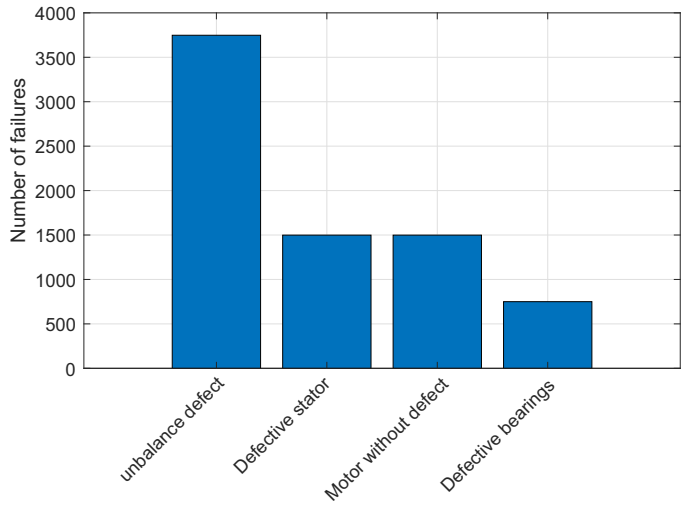

Figure 58. Number of failures classified in the 'Defect unbalance' test set.

Table 9. Performance of NARX neural network for imbalance defect.

Accuracy	Precision Total	Recall	F1 Score
0.95	1.0	0.95	0.97

5.2.3. Scenario 3—Validation of the NARX Network—Defective Bearings

For this third network-validation scenario, a new dataset made up of signals collected from the engine with damaged bearings was inserted into the NARX neural network inputs. For this type of fault, the network responded well, achieving a performance of 95%. Figures 59–61 and Table 10.

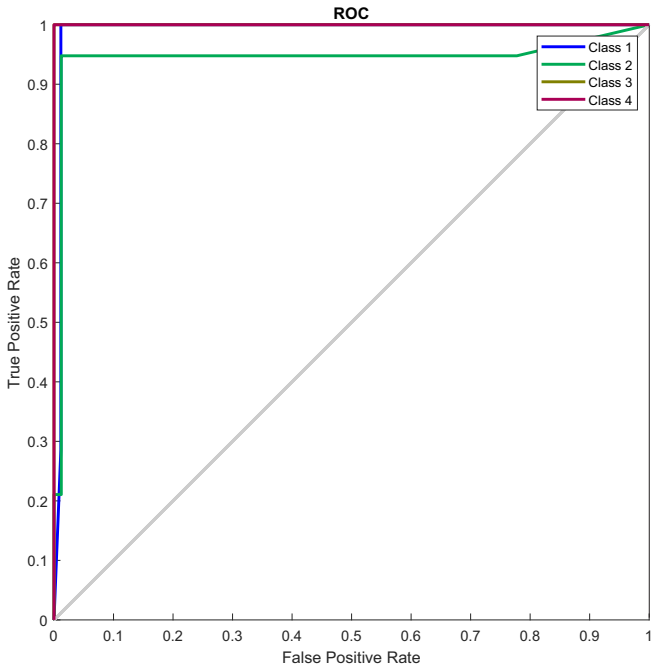

Figure 59. ROC curve of the faulty bearings test set.

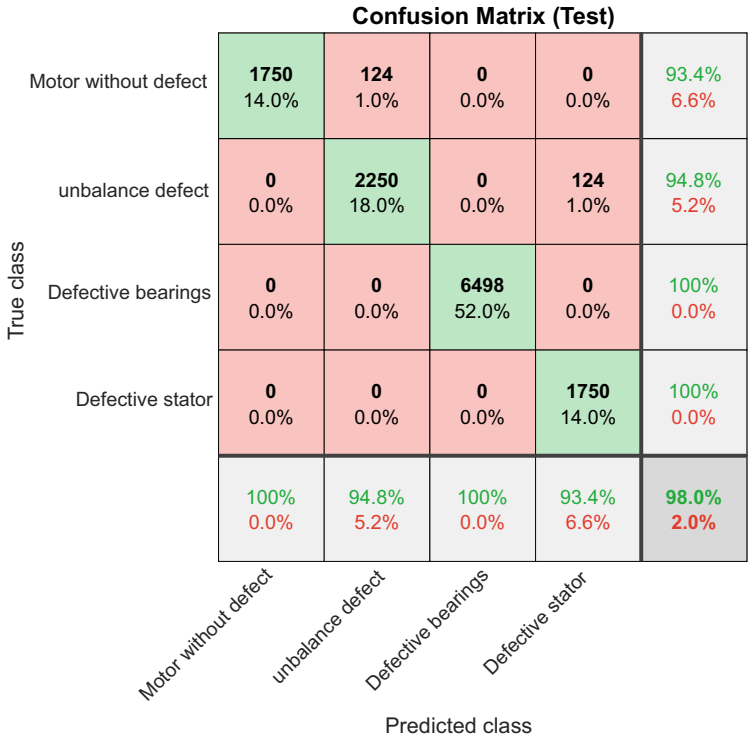

Figure 60. Confusion matrix for defective bearings.

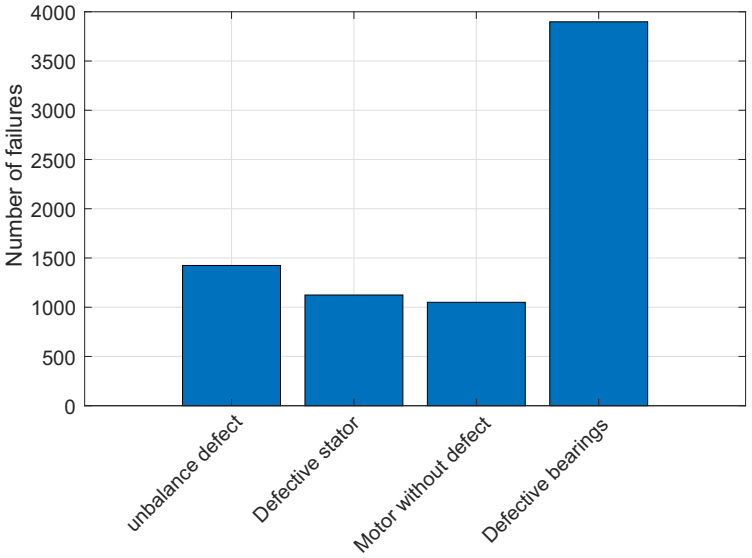

Figure 61. Classified failures for defective bearings.

Table 10. NARX neural network performance for defective bearings.

Accuracy	Precision Total	Recall	F1 Score
0.98	1.0	0.98	0.99

5.2.4. Scenario 4—Validation of the NARX Network—Faulty Stator

For this fourth network-validation scenario, a new dataset made up of signals collected from the motor with unbalanced stator phases was inserted into the inputs of the NARX neural network. For this type of fault, the network responded well, achieving a performance of 98%. Figures 62–64 and Table 11.

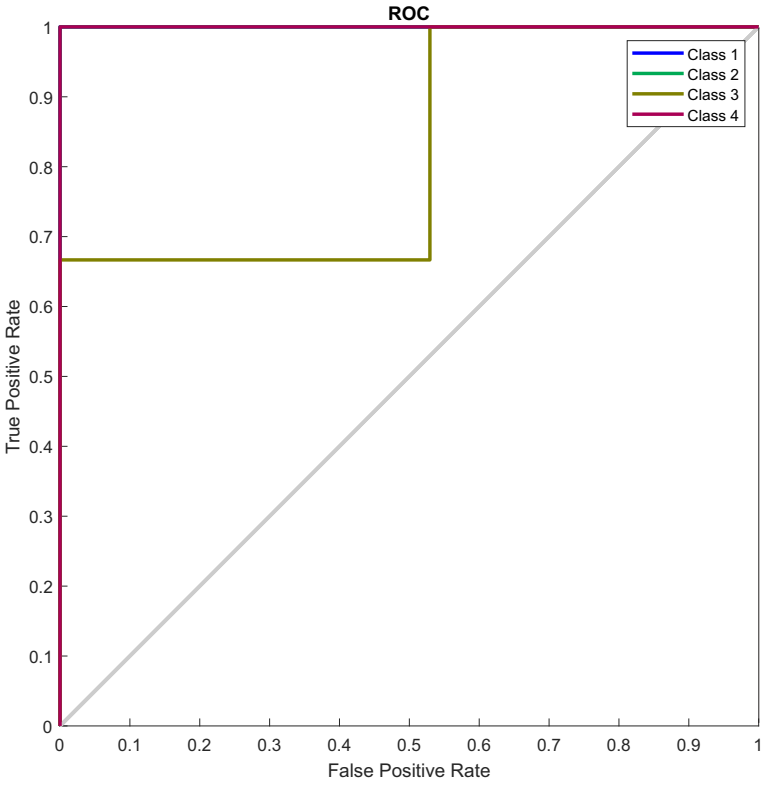

Figure 62. ROC curve for defective stator.

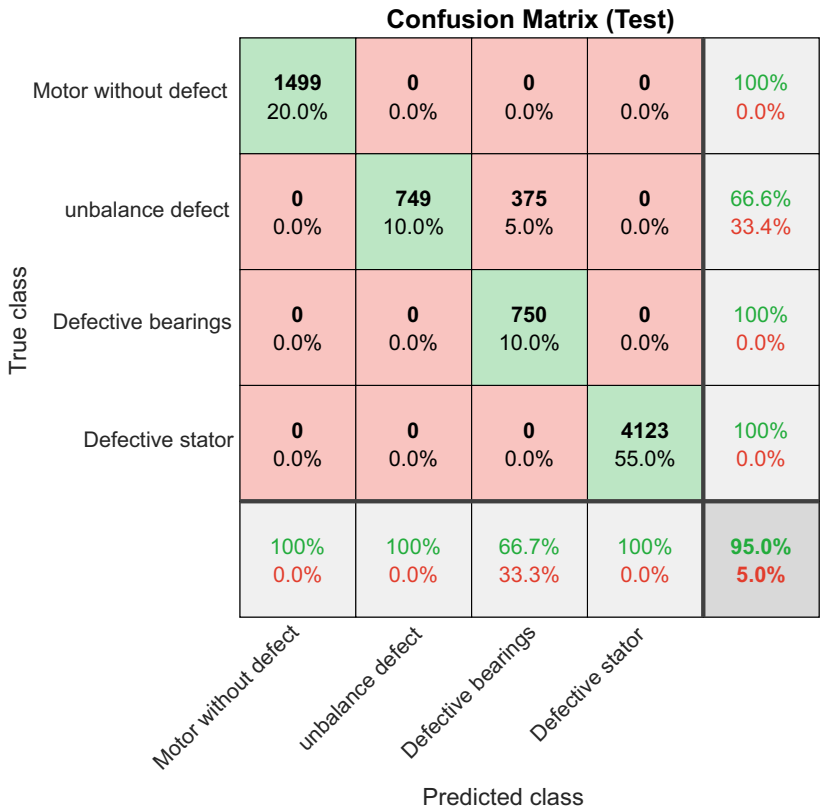

Figure 63. Confusion matrix for the defective stator.

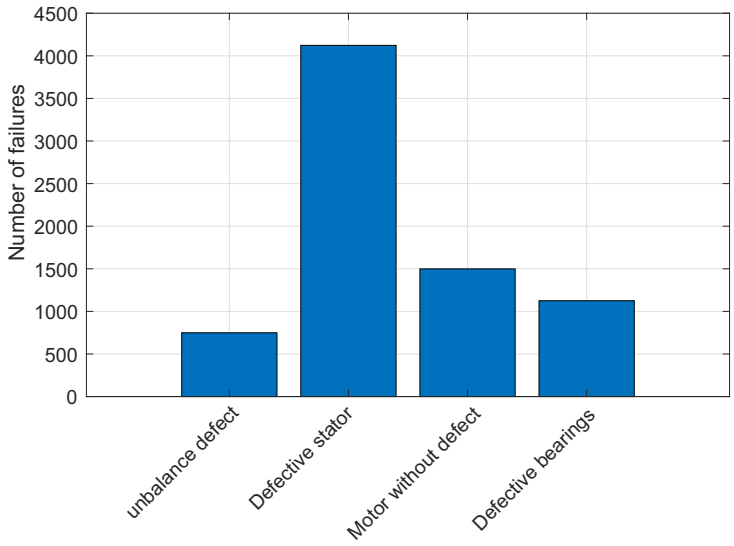

Figure 64. Faults classified for defective stator.

Table 11. Performance of NARX neural network for defective stator.

Accuracy	Precision Total	Recall	F1 Score
0.95	1.0	0.95	0.97

6. Discussion

The NARX model was used as a viable tool for diagnosing and classifying faults in three-phase induction motors. After a scanning process to find the best network, with the ideal number of neurons for the two hidden layers and the delays for the inputs and outputs, the selected network was subjected to a series of validation tests. The results of these tests showed that the network has an excellent generalization capacity in all the situations evaluated. The data obtained prove the network's excellent performance in classifying faults, even when new data are presented. Table 12 shows the hit rate for each engine condition in the four test scenarios discussed in Section 5.2.

Table 12. Performance of the NARX neural network for each type of fault classified.

Motor without Defect	Unbalanced Defect	Defective Bearings	Defective Stator
94.2%	95%	98%	95%

Comparing the Results

Various studies have investigated the application of machine learning algorithms for fault diagnosis in induction motors, presenting variations in their methodologies and results. The Multilayer Perceptron Neural Network (MLP) proposed by [17] for classifying faults in three-phase induction motors achieved an accuracy of 97%. Conversely, the SVM method used by [20] for detecting and classifying faults in three-phase induction motors within wind turbine pitch control systems achieved an overall accuracy of 98% on the training set and 96.5% on the test set.

In this context, the present study developed a Nonlinear Autoregressive Network with Exogenous Inputs (NARX) for classifying faults in three-phase induction motors, achieving an accuracy of 99% on the training set and 98% on the test set. The applied methodology included a rigorous validation process using a diverse dataset, which strengthens the reliability of the obtained results.

When comparing the results of previous studies with those of the present work, it is evident that the NARX neural network demonstrated superior performance. This increase in accuracy can be attributed to various factors such as the network structure, the quantity and diversity of the data used, and the validation process adopted. While the work of [17] demonstrated the effectiveness of the MLP and [20] evidenced the capability of the SVM, the present study highlights the superiority of the NARX neural network in the specific task of classifying faults in three-phase induction motors, and the incorporation of highly nonlinear relationships between electrical and mechanical quantities in NARX networks facilitates the classification of faults.

These quantities selected as input parameters in the NARX network define the dynamic and operational behavior of the motors, such as the engine power, temperature rise affecting the stator windings, and efficiency.

7. Conclusions

Three-phase induction motors play a crucial role in industrial processes. The proper functioning of this equipment is essential to ensure the good performance of the machines on the production line. The identification and classification of initial failures in these engines are vital to increasing efficiency, safety, reliability, and durability, thus ensuring quality production. Therefore, developing effective techniques for obtaining data and diagnosing faults in three-phase induction motors is essential. This paper focuses on the early identification of faults through the accurate diagnosis and classification of faults in three-phase induction motors using a neural network through the analysis of current, temperature, and vibration signals. The development and use of an Exogenous AutoRegressive Neural Network (NARX) for fault classification obtained satisfactory results, validating the effectiveness of the proposed method. The case study showed that the proposed method for developing a classification model using a neural network is very efficient in identifying failures in TIMs. Among the faults classified with greater accuracy, the proposed model stood out in detecting defective bearings, achieving an accuracy of 98% for new data. In this research, the neural network was developed in the Matlab® environment, which demonstrated an excellent performance. However, for future research, it is important to consider the need to adapt the code to a language that can be incorporated into embedded systems for real-time detection.

The main differences of the NARX neural network are the following:

Dynamical Systems Modeling: The NARX network is designed to model dynamical systems, where the future state of the system depends not only on current inputs but also on previous states. This characteristic is particularly important in engine analysis, where operating conditions may vary over time and failures may develop gradually. The ability to consider the history of engine states allows the NARX network to identify complex temporal patterns that other neural networks may not capture.

Inclusion of Exogenous Inputs: The NARX network can incorporate exogenous inputs, such as environmental or operational variables, that can influence engine performance. For example, ambient temperature, applied load, and other external conditions can be included in the model, providing a more holistic and accurate analysis of engine conditions.

Robustness in Prediction and Diagnosis: Due to its autoregressive structure, the NARX network is more robust in predicting and diagnosing failures, even in situations where the data are noisy or incomplete. The ability to make predictions based on historical data helps in the early identification of anomalies, enabling corrective actions before failures become critical.

Versatility and Adaptability: The NARX network can be trained for different engine types and operating conditions, making it a versatile and adaptable tool. Its flexibility allows it to be applied to a wide range of fault-diagnosis scenarios, from induction motors to direct current motors and synchronous motors.

The use of a NARX neural network in engine fault classification offers significant advantages in terms of accuracy, robustness, and dynamic systems' modeling capabili-

ties. Its ability to incorporate exogenous inputs and consider historical states makes it a powerful tool for predictive maintenance and the efficient management of electric motors. Adopting this technology can result in better fault detection, reduced maintenance costs, and increased operational reliability.

An innovative aspect of this work is the application of the NARX neural network as a multiclass classifier for failures in three-phase induction motors. NARX networks are typically used for time series forecasting, so their application in this context is relatively rare in the scientific literature. Thus, this paper makes a significant contribution to technical and scientific advancements in this field.

Author Contributions: V.G.d.A., J.M.M.V., and A.O.-S.B. conceived and designed the study; V.G.d.A., J.M.M.V., A.O.S. and D.A.d.M.F. were responsible for the methodology; V.G.d.A., A.O.-S.B., R.d.A.T., and D.A.d.M.F. performed the simulations and experiments; V.G.d.A., A.O.-S.B., J.M.M.V., E.R.L.V., R.d.A.T. and D.A.d.M.F. reviewed the manuscript and provided valuable suggestions; V.G.d.A., J.M.M.V., E.R.L.V., R.d.A.T., and D.A.d.M.F. wrote the paper; J.M.M.V. and A.O.-S.B. were responsible for supervision. All authors have read and agreed to the published version of the manuscript.

Funding: This research was funded and supported by the Coordenação de Aperfeiçoamento de Pessoal de Nível Superior—Brasil (CAPES)—Finance and Conselho Nacional de Desenvolvimento Científico e Tecnológico (CNPq).

Conflicts of Interest: The authors declare no conflicts of interest.

Abbreviations

The following abbreviations are used in this manuscript:

ANN	Artificial Neural Network
DC	Direct current
FFT	Fast Fourier Transform
FIS	Fuzzy Inference System
GA	Genetic Algorithm
IM	Induction motor
LM	Levenberg–Maquardt
ML	Machine learning
MLP	Multilayer Perceptron
MSE	Mean Square Error
NARX	Nonlinear AutoRegressive Exogenous inputs
RNN	Recurrent neural network
SVM	Support vector machine
TIM	Three-phase induction motor

References

1. Graciola, C.L.; Goedtel, A.; Castoldi, M.F.; Gentil, M.G.; Souza, W.A.; Vitor, A.L.O. An Efficiency Study of a Three-Phase Induction Motor Through Predictive Control Strategies. In Proceedings of the 2023 15th IEEE International Conference on Industry Applications (INDUSCON), São Bernardo do Campo, Brazil, 22–24 November 2023; pp. 899–905. [CrossRef]
2. Santos, M.S.; Paz, E.H.; Aguiar, V.B.; Pontes, R.T. Non-invasive monitoring system for analysis of energy efficiency of three-phase induction motors. In Proceedings of the 2022 Workshop on Communication Networks and Power Systems (WCNPS), Fortaleza, Brazil, 17–18 November 2022; pp. 1–6. [CrossRef]
3. Ojaghi, M.; Mohammadi, M. Modeling eccentricity faults with axial asymmetry in three-phase induction motors. In Proceedings of the IECON 2016—42nd Annual Conference of the IEEE Industrial Electronics Society, Florence, Italy, 23–26 October 2016; pp. 1524–1529. [CrossRef]
4. Alsaedi, M.A. Fault diagnosis of three-phase induction motor: A review. *Optics* **2015**, *4*, 1–8. [CrossRef]
5. Sheikh, A.; Bakhsh, S.; Irfan, M.; Nor, N.; Nowakowski, G. A Review to Diagnose Faults Related to Three-Phase Industrial Induction Motors. *J. Fail. Anal. Prev.* **2022**, *22*, 1546–1557. [CrossRef]
6. Broniera, P.J.; Gongora, W.S.; Goedtel, A.; Godoy, W.F. Diagnosis of stator winding inter-turn short circuit in three-phase induction motors by using artificial neural networks. In Proceedings of the 2013 9th IEEE International Symposium on Diagnostics for Electric Machines, Power Electronics and Drives (SDEMPED), Valencia, Spain, 27–30 August 2013; pp. 281–287. [CrossRef]

7. Okpo, E.E.; Le Roux, P.F.; Nnachi, A.F. Induction Motor Fault Identification using Support Vector Machine. In Proceedings of the 2023 6th International Conference on Renewable Energy and Power Engineering (REPE), Beijing, China, 15–17 September 2023; pp. 168–174. [CrossRef]
8. Narwade, S.; Kulkarni, P.; Partil, C. Fault detection of induction motor using current and vibration monitoring. *Int. J. Adv. Comput. Res.* **2013**, *3*, 272.
9. Almounajjed, A.; Sahoo, A.K.; Kumar, M.K. Diagnosis of stator fault severity in induction motor based on discrete wavelet analysis. *Measurement* **2021**, *182*, 109780. [CrossRef]
10. Xuhong, W.; Yigang, H. Diagonal recurrent neural network based on-line stator winding turn fault detection for induction motors. In Proceedings of the 2005 International Conference on Electrical Machines and Systems, Nanjing, China, 27–29 September 2005; Volume 3, pp. 2266–2269.
11. Aydin, I.; Karakose, M.; Akin, E. Artificial immune based support vector machine algorithm for fault diagnosis of induction motors. In Proceedings of the 2007 International Aegean Conference on Electrical Machines and Power Electronics, Bodrum, Turkey, 10–12 September 2007; pp. 217–221.
12. Cho, H.C.; Knowles, J.; Fadali, M.S.; Lee, K.S. Fault detection and isolation of induction motors using recurrent neural networks and dynamic Bayesian modeling. *IEEE Trans. Control. Syst. Technol.* **2009**, *18*, 430–437. [CrossRef]
13. Ramalho, G.L.B.; Pereira, A.H.; Rebouças Filho, P.P.; Medeiros, C.M.d.S. Detecção de falhas em motores elétricos através da classificação de padrões de vibração utilizando uma rede neural ELM. *Holos* **2014**, *4*, 185–194. [CrossRef]
14. Vitor, A.L.O.; Oliveira, F.M.; Ronqui, L.A.; Goedtel, A.; Scalassara, P.R.; Silva, S.A.O.; Vallim, M.B.R. Detecção de falhas elétricas em motores de indução utilizando rede radial basis function. *An. Congr. Bras. Automá Tican* **2014**, *46*, 37–42.
15. Jagadanand, G.; Dias, F.L. ARM based induction motor fault detection using wavelet and support vector machine. In Proceedings of the 2015 IEEE International Conference on Signal Processing, Informatics, Communication and Energy Systems (SPICES), Kozhikode, India, 19–21 February 2015; pp. 1–4.
16. Sobrinho, C.A.N.; Lima Filho, A.C.; de Sena, A.P.C.; Brito, J.N.; da Silva, J.F.; Mafaldo, M. Wavelet Transform for detecting broken bars in Three-Phase Induction Motors. *Principia Mag. IFPB Sci. Technol. Dissem.* **2018**, *42*, 72–83.
17. Gongora, W.S.; Goedtel, A.; da Silva, S.A.O.; Graciola, C.L. Neural approach to fault detection in three-phase induction motors. *IEEE Lat. Am. Trans.* **2016**, *14*, 1279–1288. [CrossRef]
18. Liu, R.; Yang, B.; Zio, E.; Chen, X. Artificial intelligence for fault diagnosis of rotating machinery: A review. *Mech. Syst. Signal Process.* **2018**, *108*, 33–47. [CrossRef]
19. Ding, A.; Yi, X.; Qin, Y.; Wang, B. Self-driven continual learning for class-added motor fault diagnosis based on unseen fault detector and propensity distillation. *Eng. Appl. Artif. Intell.* **2024**, *127*, 107382. [CrossRef]
20. Kandukuri, S.T.; Senanyaka, J.S.L.; Robbersmyr, K.G. A two-stage fault detection and classification scheme for electrical pitch drives in offshore wind farms using support vector machine. *IEEE Trans. Ind. Appl.* **2019**, *55*, 5109–5118. [CrossRef]
21. WEG Specification Guide: Electric Motors. In Portuguese Language. 2023.
22. Guedes, J.J.; Goedtel, A.; Castoldi, M.F.; Sanches, D.S.; Serni, P.J.A.; Rezende, A.F.F.; Bazan, G.H.; de Souza, W.A. Three-phase induction motor fault identification using optimization algorithms and intelligent systems. In *Soft Computing*; Springer: Berlin/Heidelberg, Germany, 2024; pp. 1–16.
23. Silva, M.A.; Lucena-Junior, J.A.; da Silva, J.C.; Belo, F.A.; Lima-Filho, A.C.; Ramos, J.G.G.d.S.; Camara, R.; Brito, A. Sensorless Speed Estimation of Induction Motors through Signal Analysis Based on Chaos Using Density of Maxima. *Entropy* **2024**, *26*, 361. [CrossRef] [PubMed]
24. Lucas, G.B.; de Castro, B.A.; Rocha, M.A.; Andreoli, A.L. Three-phase induction motor loading estimation based on Wavelet Transform and low-cost piezoelectric sensors, Measurement. *Measurement* **2020**, *164*, 107956. [CrossRef]
25. Oliveira, R.F. *Artificial Intelligence in Portuguese*; Educational Publisher and Distributor S.A.: Londrina, Brazil, 2018.
26. Santos, G.R.; Brito, J.N.; Santana, C.; Lara, H. Monitoring of three-phase motors through artificial intelligence. In *Anais do XVIII Congresso Nacional de Engenharia Mecânica e Industrial*; Embra Embra Serviços em Tecnologia Ltda EPP: Campinas, Brazil, 2018; Volume 2.
27. Preethi, I.; Suryaprakash, S.; Mathankumar, M. A State-of-Art Approach on Fault Detection in Three Phase Induction Motor using AI Techniques. In Proceedings of the 2021 5th International Conference on Computing Methodologies and Communication (ICCMC), Erode, India, 8–10 April 2021; pp. 567–573. [CrossRef]
28. Mohamed, M.; Mohamed, E.; Mohamed, A.A.; Abdel-Nasser, M.; Hassan, M.M. Detection of Inter Turn Short Circuit Faults in Induction Motor using Artificial Neural Network. In Proceedings of the 2020 26th Conference of Open Innovations Association (FRUCT), Yaroslavl, Russia, 20–24 April 2020; pp. 297–304. [CrossRef]
29. Aquize, R.; Cajahuaringa, A.; Machuca, J.; Mauricio, D.; Mauricio Villanueva, J.M. System Identification Methodology of a Gas Turbine Based on Artificial Recurrent Neural Networks. *Sensors* **2023**, *23*, 2231. [CrossRef] [PubMed]
30. Khaled, S.; Fakhry, M.; Mubarak, A.S. Classification of pcg signals using a nonlinear autoregressive network with exogenous inputs (narx). In Proceedings of the 2020 International Conference on Innovative Trends in Communication and Computer Engineering (ITCE), Aswan, Egypt, 8–9 February 2020; pp. 98–102.
31. de Pádua Braga, A.; de Leon Ferreira, A.C.P.; Ludermir, T.B. *Artificial Neural Networks: Theory and Applications*; LTC Publisher: Hong Kong, China, 2007. (In Portuguese)

32. Junior, G.B.V.; Lima, B.N.; Pereira, A.A.; Rodrigues, M.F.; Oliveira, J.R.L.; Silio, L.F.; Carvalho, A.S.; Ferreira, H.R.; Passos, R.P. Métricas utilizadas para avaliar a eficiência de classificadores em algoritmos inteligentes. *Rev. Cpaqv-Centro Pesqui. Avançadas Qual. Vida* **2022**, *14*, 2.
33. Polo, T.C.F.; Miot, H.A. Applications of the ROC curve in clinical and experimental studies. *J. Vasc. Bras.* **2020**, 1–4.
34. César da Silva, J.; Lima, T.L.d.V.; Lucena Júnior, J.A.d.; Lyra, G.J.; Souto, F.V.; Pimentel, H.d.S.; Belo, F.A.; Lima Filho, A.C. Non-Invasive Method for In-Service Induction Motor Efficiency Estimation Based on Sound Acquisition. *Appl. Sci.* **2020**, *10*, 3757. [CrossRef]